The Plant Cell, Vol. 32: 166–185, January 2020, www.plantcell.org © 2020 ASPB.

Oxylipins Other Than Jasmonic Acid Are Xylem-Resident Signals Regulating Systemic Resistance Induced by *Trichoderma virens* in Maize

Ken-Der Wang, Eli J. Borrego,[1] Charles M. Kenerley, and Michael V. Kolomiets[2]

Department of Plant Pathology and Microbiology, Texas A&M University, College Station, Texas 77843

ORCID IDs: 0000-0003-4204-5496 (K.-D.W.); 0000-0002-3538-3203 (E.J.B.); 0000-0002-4547-4635 (C.M.K.); 0000-0003-1038-9534 (M.V.K.)

Multiple long-distance signals have been identified for pathogen-induced systemic acquired resistance, but mobile signals for symbiont-induced systemic resistance (ISR) are less well understood. We used ISR-positive and -negative mutants of maize (*Zea mays*) and the beneficial fungus *Trichoderma virens* and identified 12-oxo-phytodienoic acid (12-OPDA) and α-ketol of octadecadienoic acid (KODA) as important ISR signals. We show that a maize 13-lipoxygenase mutant, *lox10*, colonized by the wild-type *T. virens* (TvWT) lacked ISR response against *Colletotrichum graminicola* but instead displayed induced systemic susceptibility. Oxylipin profiling of xylem sap from *T. virens*–treated plants revealed that 12-OPDA and KODA levels correlated with ISR. Transfusing sap supplemented with 12-OPDA or KODA increased receiver plant resistance in a dose-dependent manner, with 12-OPDA restoring ISR of *lox10* plants treated with TvWT or *T. virens Δsm1*, a mutant unable to induce ISR. Unexpectedly, jasmonic acid (JA) was not involved, as the JA-deficient *opr7 opr8* mutant plants retained the capacity for *T. virens*–induced ISR. Transcriptome analysis of TvWT-treated maize B73 revealed upregulation of 12-OPDA biosynthesis and OPDA-responsive genes but downregulation of JA biosynthesis and JA response genes. We propose a model that differential regulation of 12-OPDA and JA in response to *T. virens* colonization results in ISR induction.

INTRODUCTION

Within the rhizosphere, plants must discern beneficial microbes from pathogens and respond accordingly by dampening host defenses when colonized by beneficial microbes or heightening defenses against pathogens (Heil and Bostock, 2002; Katagiri and Tsuda, 2010). One such response to beneficial microorganisms is heightened resistance to a wide range of pathogens, a phenomenon termed induced systemic resistance (ISR). ISR is triggered following root colonization by beneficial microbes, and it results in priming of rapid and robust defense responses against future pathogen infections (Pieterse et al., 2014b). While the primed plants display strong systemic resistance upon infection, they display little to no discernable changes in their defense status in the absence of pathogens (Wang et al., 2005; Conrath et al., 2006; Pieterse et al., 2014a). The mechanisms by which these beneficial microbes enhance both plant growth and defenses remain a mystery (Havko et al., 2016). The specific signaling mechanisms of ISR are much less understood compared with the pathogen-triggered systemic acquired resistance. While systemic acquired resistance (SAR) relies mostly on salicylic acid (SA) signaling (Pieterse et al., 2014b), the mobile signals responsible include azelaic acid, pipecolic acid, methyl salicylate, glycerol-3-P, and dehydroabietinal (Klessig et al., 2018). ISR induction is postulated to require jasmonic acid (JA) and ethylene signaling in an SA-independent manner (Pieterse et al., 2014a); however, SA has also been implicated in ISR signaling for certain species (Knoester et al., 1999; Korolev et al., 2008; Pozo et al., 2008; Salas-Marina et al., 2011).

Trichoderma spp are soil-borne filamentous fungi found ubiquitously, including agriculturally relevant *Trichoderma virens* and *Trichoderma harzianum*. They have been studied extensively for their beneficial effects on plants, such as enhancing growth of shoots and roots, interacting directly via antimicrobial activity against soil-borne pathogens through antibiosis and mycoparasitism, and triggering ISR (Yedidia et al., 1999; Howell et al., 2000; Lorito et al., 2010; Druzhinina et al., 2011; Hermosa et al., 2012). *T. virens*–induced ISR against diverse pathogens was demonstrated in several plant species including Arabidopsis (*Arabidopsis thaliana*), cotton (*Gossypium hirsutum*), tomato (*Solanum lycopersicum*), and maize (*Zea mays*; Djonović et al., 2006, 2007; Contreras-Cornejo et al., 2011).

The signal communication between *Trichoderma* and host plants that results in ISR is poorly understood; however, a plethora of fungal molecules have been identified that trigger or suppress ISR. Sm1, a small secreted protein from *T. virens*, plays an integral role in ISR signaling. The *Δsm1* mutant can no longer trigger ISR in either maize or cotton, while the strains overexpressing *SM1* enhance plant resistance against pathogens to levels greater than the wild-type *T. virens* (TvWT; Djonović et al., 2006, 2007). Similarly, Epl1, a homolog of Sm1 in *Trichoderma atroviride*, induces ISR in tomato and improves resistance against bacterial and fungal pathogens (Salas-Marina et al., 2015). *T. virens* also

[1] Current address: Thomas H. Gosnell School of Life Sciences, Rochester Institute of Technology, Rochester, New York 14623
[2] Address correspondence to kolomiets@tamu.edu.
The authors responsible for distribution of materials integral to the findings presented in this article in accordance with the policy described in the Instructions for Authors (www.plantcell.org) are: Charles M. Kenerley (c-kenerley@tamu.edu) and Michael V. Kolomiets (kolomiets@tamu.edu).
www.plantcell.org/cgi/doi/10.1105/tpc.19.00487

IN A NUTSHELL

Background: *Trichoderma virens* is an agriculturally-relevant root-colonizing fungus that provides its plant hosts many benefits, such as increased growth, destruction of soil-borne pathogens, and enhanced systemic resistance against foliar pathogens, termed induced systemic resistance (ISR). The mobile ISR signals are not known, though it is postulated to involve phytohormones jasmonic acid (JA) and ethylene. JA is one of hundreds of oxylipins, which are hypothesized to regulate many physiological processes including ISR. Lipoxygenases (LOX) are key enzymes in the biosynthesis of oxylipins. Previously, we identified maize root-expressed LOX3 as a negative regulator of ISR, because *lox3* knock-out mutants displayed strong constitutive ISR. Additionally, we identified *T. virens* mutants that either cannot trigger ISR or trigger a stronger systemic response.

Question: We hypothesized that signals other than JA are responsible for ISR, which originate in the roots and are transported through the plant vasculature. By utilizing ISR-positive and -negative mutants of both maize (*Zea mays*) and *T. virens*, we profiled xylem sap of *T. virens*-treated maize to identify potential ISR signals.

Findings: Here, LOX10 was identified as a positive regulator of ISR, as instead of conferring ISR, *T. virens*-colonized *lox10* mutants became more susceptible to leaf pathogens. Metabolite profiling was performed on xylem saps collected from *lox3* and *lox10* mutants treated with ISR-positive or ISR-negative strains of *T. virens*. The screening revealed that accumulation of two oxylipins, the JA precursor, 12-OPDA, and α-ketol, KODA, correlated with ISR activation. Sap transfusion of either of these two compounds enhanced ISR of receiver plants against infection in a dose-dependent manner. Surprisingly, transfusion with JA increased susceptibility to infection. Furthermore, JA-deficient mutants still benefited from *T. virens*-triggered ISR.

Next steps: While 12-OPDA biosynthesis is well understood, specific maize enzymes for KODA biosynthesis are unknown. Our future work will focus on screening available maize mutants to identify enzymes responsible for KODA biosynthesis. It will also be of interest to identify receptors for 12-OPDA and KODA that, when bound, trigger ISR.

secretes several other peptides that function as negative regulators of ISR. For example, deletion of Suppressor of Induced Resistance (*SIR1*; protein ID 77560) greatly enhanced ISR of maize against a necrotrophic pathogen, *Cochliobolus heterostrophus*, the causal agent of Southern corn leaf blight (Lamdan et al., 2015). The specific mechanisms by which these secreted peptides regulate ISR remain unknown. We previously showed that one function of Sm1 is to regulate synthesis of maize oxylipins with signaling properties (Constantino et al., 2013).

Oxylipins are a large group of oxidized lipid signals that regulate many physiological processes, such as growth and development, defense responses to pathogens and herbivores, and abiotic stresses (Borrego and Kolomiets, 2016). They are mainly produced through enzymatic oxygenation of polyunsaturated fatty acids, linoleic acid (C18:2), and linolenic acid (C18:3) at the carbon position 9 or 13 by 9- or 13-lipoxygenase (LOX), respectively (Feussner and Wasternack, 2002; Andreou et al., 2009). The primary products of LOX reactions are fed into several enzyme branches, resulting in the biosynthesis of more than 650 structurally and functionally diverse oxylipins (Borrego and Kolomiets, 2016). Undoubtedly, the best-characterized oxylipin in terms of relevance to ISR is JA. JA biosynthesis begins in plastids, where 13-LOX, allene oxide synthase (AOS), and allene oxide cyclase (AOC) produce JA precursor 12-oxo-phytodienoic acid (12-OPDA). 12-OPDA is transported to the peroxisome and converted to JA. JA is further conjugated to Ile by JAR1 to produce JA-Ile, the biologically active jasmonate that binds as a ligand to the CORONATINE INSENSITIVE1 (COI1)-JASMONATE ZIM DOMAIN (JAZ) receptor complex to activate downstream JA responses.

While the functions of JA are well documented, the physiological roles of the vast majority of other oxylipins, especially the 9-LOX–derived metabolites, collectively called 9-oxylipins, are largely unknown (Borrego and Kolomiets, 2016). The negative role of 9-LOX activity in regulating ISR has been demonstrated by examination of the maize *lox3-4* mutant. This strong loss-of-function mutant demonstrated increased resistance against various seed, stalk, root, and foliar pathogens (Gao et al., 2007; Isakeit et al., 2007). Roots of *lox3-4* mutant over-accumulated defense hormones JA, ethylene, and SA and overexpressed many defense genes (Gao et al., 2008). Expression of *LOX3* has been observed exclusively in maize roots and has been shown to be suppressed by *T. virens* in a Sm1-dependent manner (Constantino et al., 2013). Furthermore, stem transfusion with xylem sap derived from *lox3-4* roots to the wild-type maize confers systemic resistance against *Colletotrichum graminicola*, proving that a systemic resistance signal(s) originates from roots and travels systemically through the xylem (Constantino et al., 2013). Because LOX3-deficient mutants overexpress several JA biosynthesis genes including *LOX10* (Gao et al., 2008), we hypothesized that constitutively active ISR in the *lox3-4* mutant is due to overexpression of *LOX10* and overproduction of JA or other oxylipins. Maize *lox10* mutants are green leaf volatile deficient and accumulate significantly lower wound-induced levels of 12-OPDA and JA in leaves (Christensen et al., 2013).

In support of this hypothesis, here we showed that LOX10 function is indeed required to establish proper ISR, as instead of increased resistance to leaf pathogens, colonization of *lox10* mutant roots by *T. virens* resulted in increased susceptibility. Oxylipin and hormone profiling of xylem sap from the wild-type maize, *lox3*, and *lox10* mutants treated with either the wild type or ISR-perturbed *T. virens* mutants, along with pharmacological treatments indicated that 12-OPDA, produced by LOX10, and the α-ketol 9-hydroxy-10-oxo-12(*Z*),15(*Z*)-octadecadienoic acid (KODA), produced by an unknown 9-LOX, are major ISR long-distance signals. Unexpectedly, the JA-deficient *opr7 opr8* double mutant displayed normal ISR response induced by *T. virens*, suggesting

that JA is dispensable for ISR signaling in maize. Taken together, our results present evidence that the JA precursor, 12-OPDA, and KODA, but not JA, are xylem-resident signals required for ISR induction in maize.

RESULTS

T. virens Induces *LOX10* Expression at the Early Stages of Interaction

To assess the involvement of LOX10 in maize–*T. virens* interactions, B73 seedlings were grown in hydroponic conditions and subsequently treated with TvWT, *Δsm1*, or *Δsir1*. These three strains have different abilities to induce ISR in maize. Compared with TvWT, *Δsm1* is unable to induce ISR (Djonovic et al., 2007), whereas *Δsir1* induces exceptionally strong ISR against *C. heterostrophus*, a necrotrophic pathogen and causal agent of Southern corn leaf blight (Lamdan et al., 2015). Treatment with the TvWT strain resulted in the upregulation of *LOX10* expression as early as 3 and 6 h, ranging between three- and fourfold induction compared to untreated plants (Figure 1A). This effect was diminished by 9 h, suggesting that *LOX10* induction is transient. Interestingly, *Δsir1* induced *LOX10* earlier than TvWT at 2 h after treatment. By contrast, the *Δsm1* strain was unable to induce transcript accumulation at any time point, suggesting that *LOX10* expression is dependent on functional Sm1 protein.

We further tested accumulation of LOX10 protein by taking advantage of a publicly available transgenic maize line expressing stable LOX10-yellow fluorescent protein (YFP) driven by the native *LOX10* promoter (Mohanty et al., 2009). When the transgenic seedlings were treated with TvWT, they accumulated substantially greater levels of the fusion protein in the developing lateral roots compared to untreated plants (Figure 1B). Together, these results suggested that *LOX10* expression was induced at both the transcript and protein levels and that induction is positively regulated by Sm1 but negatively regulated by Sir1.

To determine whether the more robust induction of *LOX10* expression by *Δsir1* was due to altered expression of *SM1*, transcript accumulation of *SM1* and *SIR1* was measured by qPCR in TvWT and both mutants at 6 h after transfer to hydroponic conditions. Expression of *SM1* was threefold greater in *Δsir1* mutant compared to TvWT, whereas *SIR1* expression in *Δsm1* was not altered (Figure 1C). Expression of *SM1* and *SIR1* at 30 h mirrored that seen at 6 h (data not shown). These results indicate that a likely reason for *Δsir1* being more effective in induction of *LOX10* is due to increased expression of *SM1* in this mutant and confirm that *LOX10* is indeed one host target positively regulated by Sm1 to promote ISR.

LOX10 Is Required for *T. virens*–Mediated ISR

To further define the role of LOX10 in regulating maize–*T. virens* interactions, the B73 inbred line and near-isogenic *lox10* mutant alleles, *lox10-2* and *lox10-3*, were treated with TvWT and assessed for ISR response against pathogen infection. As expected, TvWT-treated B73 displayed characteristic ISR response, as evidenced by significant reduction of lesion areas and chlorosis

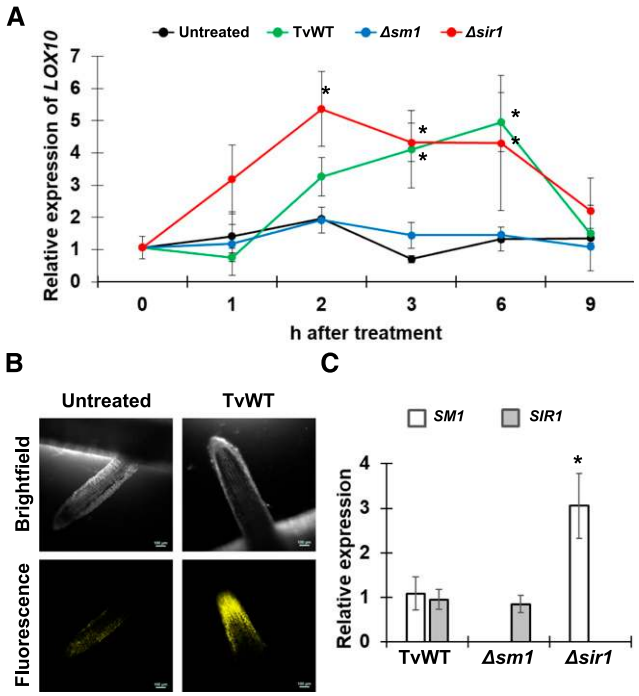

Figure 1. *LOX10* Expression Is Induced by *T. virens* in a Sm1-Dependent Manner.

(A) Expression of *LOX10* by qPCR was determined in seedling roots of B73 after treatment with *T. virens* strains, TvWT, ISR-deficient strain *Δsm1*, or ISR-enhancing strain *Δsir1*, at 0, 1, 2, 3, 6, and 9 h after treatment and compared with untreated plants. Expression was calculated from cycle threshold values using the $2^{-\Delta\Delta Ct}$ method and normalized to transcript levels of α-*Tubulin*, and relative expression is the fold change relative to untreated plants at time 0 h. Points represent means ± SE ($n = 3$ biological replicates of plants grown in hydroponic jars, each consisting of five maize seedlings). Statistical significance was determined with Tukey's HSD test compared with untreated plants (*$P < 0.05$, **$P < 0.01$).

(B) Confocal microscopic detection of accumulation of LOX10-YFP fusion protein, driven by the endogenous *ZmLOX10* promoter, in the newly formed lateral roots of transgenic maize after treatment with TvWT compared with untreated roots. Bars = 100 μm.

(C) Expression of *SM1* and *SIR1* by qPCR was determined in *T. virens* hyphal tissue grown in MS medium. Expression was calculated from cycle threshold values using the $2^{-\Delta\Delta Ct}$ method and normalized to transcript levels of *Actin*. Bars represent means ± SE ($n = 3$ biological replicates of *T. virens* mycelia grown in hydroponic jars) relative to TvWT. Statistical significance was determined with Tukey's HSD test (*$P < 0.05$). These experiments were repeated at least two times with similar results.

caused by *C. graminicola* (Figures 2A and 2B). As previously reported, both untreated *lox10-3* and *lox10-2* mutant alleles were significantly more resistant to *C. graminicola* (Christensen, 2009). Surprisingly, instead of the ISR observed with B73, *T. virens* treatment of both *lox10* mutants resulted in significantly increased susceptibility, which we termed induced systemic susceptibility (ISS; Figures 2C and 2D). To test whether the ISS phenotype can be observed in a different genetic background of the maize inbred line, W438 inbred and near-isogenic line *lox10-3* mutant in the W438 background were treated with TvWT and challenged with

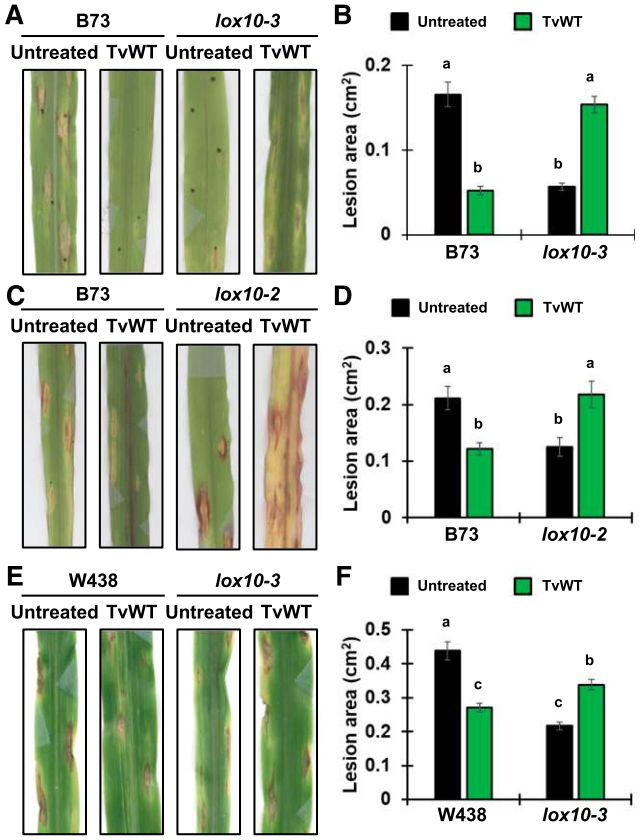

Figure 2. *LOX10* Acts as a Positive Regulator of *T. virens*-Triggered ISR against the Hemibiotrophic Pathogen *C. graminicola*.

(A) and **(B)** Visual representation of disease development **(A)** and lesion area **(B)** caused by *C. graminicola* on the leaves of untreated or TvWT-treated B73 or *lox10-3* mutant plants.
(C) and **(D)** Visual representation of disease development **(C)** and lesion area **(D)** caused by *C. graminicola* on the leaves of untreated or TvWT-treated B73 or *lox10-2* mutant plants.
(E) and **(F)** Visual representation of disease development **(E)** and lesion area **(F)** caused by *C. graminicola* on the leaves of untreated or TvWT-treated W438 or *lox10-3* mutant plants.
Infected leaves were scanned and measured using ImageJ software to determine mean lesion area. Bars represent means ± SE of the mean ($n = 5$ maize plants as biological replicates), with letters indicating significant differences among all treatments (Tukey's HSD test, $P < 0.05$). These experiments were repeated at least three times with similar results.

C. graminicola. The results reflected those observed in B73; specifically, untreated *lox10-3* was more resistant than untreated W438, but TvWT-treated *lox10-3* became significantly more susceptible (Figures 2E and 2F).

ISR is effective against a broad range of pathogens. Because *C. graminicola* is a hemibiotroph, we tested whether LOX10 is required for ISR against a necrotroph. For this, B73 and both *lox10* mutant alleles were treated with TvWT and infected with *C. heterostrophus*. Similar to *C. graminicola*, disease severity caused by *C. heterostrophus* was reduced in *T. virens*–colonized B73 and untreated *lox10-3* and *lox10-2* (Figures 3A to 3D). Furthermore, TvWT-treated *lox10-3* and *lox10-2* mutants displayed ISS, as evidenced by significantly larger lesions compared to untreated plants. ISS was also observed in TvWT-treated *lox10-3* mutant in the W438 genetic background (Figures 3E and 3F). These results suggest that LOX10 plays an essential positive regulatory role in *T. virens*–triggered ISR against both hemibiotrophic and necrotrophic pathogens.

To determine whether the *lox10* ISS phenotype may be due to insufficient root colonization by *T. virens*, we quantified maize root colonization by *T. virens* by plating TvWT-treated B73 and *lox10-3* roots on selective media and enumerating colony-forming units per total root biomass. Surprisingly, *lox10-3* roots were colonized at a greater level compared to B73 roots (Supplemental Figure 1A).

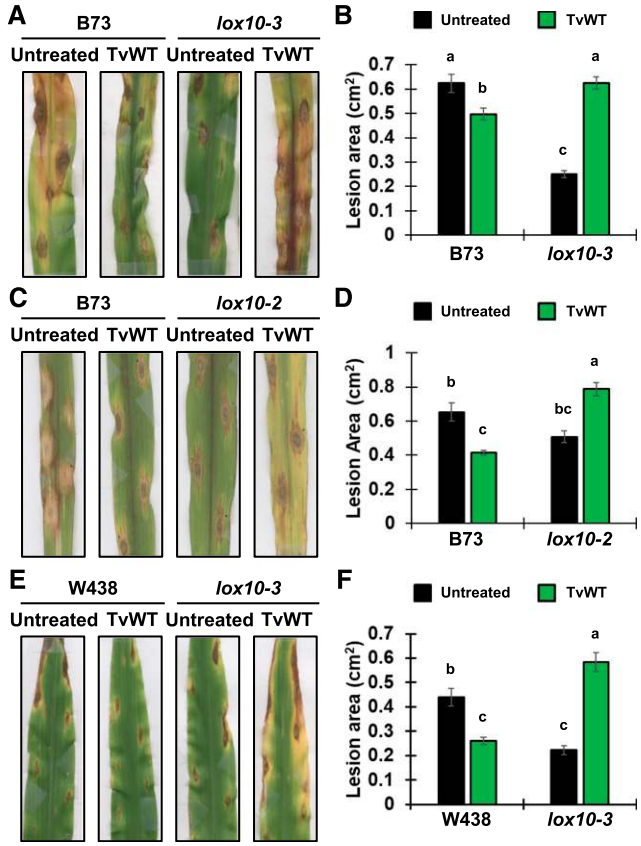

Figure 3. *LOX10* Acts as a Positive Regulator of *T. virens*–Triggered ISR against the Necrotrophic Pathogen *C. heterostrophus*.

(A) and **(B)** Visual representation of disease development **(A)** and lesion area **(B)** caused by *C. heterostrophus* on the leaves of untreated or TvWT-treated B73 or *lox10-3* mutant plants.
(C) and **(D)** Visual representation of disease development **(C)** and lesion area **(D)** caused by *C. heterostrophus* on the leaves of untreated or TvWT-treated B73 or *lox10-2* mutant plants.
(E) and **(F)** Visual representation of disease development **(E)** and lesion area **(F)** caused by *C. heterostrophus* on the leaves of untreated or TvWT-treated W438 or *lox10-3* mutant plants.
Infected leaves were scanned and measured using ImageJ software to determine mean lesion area. Bars represent means ± SE of the mean ($n = 5$ maize plants as biological replicates), with letters indicating significant differences among all treatments (Tukey's HSD test, $P < 0.05$). These experiments were repeated at least three times with similar results.

Next, we tested whether increased colonization of *lox10* mutant roots had detrimental effects on growth promotion by *T. virens*. In spite of the over-colonization, *lox10-3* plants treated with TvWT, *Δsm1*, or *Δsir1* were not negatively impacted in growth or development by any of these strains. We concluded that *T. virens* plant growth promotion was not affected by the LOX10 mutation (Supplemental Figures 1B and 1C).

T. virens–Triggered ISS in *lox10* Mutant Is Mediated by Both Host *LOX3* and Fungal *Sir1* Genes

Because the *lox3-4* mutant overexpressed *LOX10* in root tissue (Gao et al., 2007) and displayed enhanced resistance against *C. graminicola* in either the presence or absence of the TvWT treatment (Constantino et al., 2013), we hypothesized that overexpression of *LOX10* was responsible for constitutive ISR in *lox3* mutant. To test this hypothesis, we created the *lox3 lox10* double mutant (*lox3-4 lox10-3*) in B73 background at the backcross seven (BC_7) genetic stage. The *lox3 lox10* double mutant was morphologically indistinguishable from the *lox3-4* mutant (data not shown). While the untreated double mutant displayed similar to *lox3-4* resistance level, TvWT-treated *lox3 lox10* did not display the ISS phenotype observed in TvWT-treated *lox10-3*, suggesting that ISS in *lox10* mutants was dependent on functional LOX3 (Figure 4).

Additionally, we tested the role of the fungal peptide regulators of ISR, Sm1 and Sir1, in conferring the ISS phenotype of *lox10-3* mutants. As expected, there was no observed ISR in B73 colonized by *Δsm1* (Figure 4), while *Δsir1* treatment conferred enhanced ISR against *C. graminicola* to greater levels than TvWT. Surprisingly, treatment with either *Δsm1* or *Δsir1* increased susceptibility of *lox3-4*, suggesting that Sm1 may be involved in more than suppression of *LOX3* expression (Constantino et al., 2013). While both TvWT and *Δsm1* treatments resulted in increased susceptibility in *lox10-3*, *Δsir1* had no such effect. The loss of ISS triggered by *Δsir1* may suggest that functional Sir1 in *T. virens* is the primary elicitor of ISS in *lox10-3* mutant. The phenotypes of *Δsm1*- and *Δsir1*-treated *lox3 lox10* resembled that of B73, suggesting that an imbalance of either LOX3 or LOX10 may be causing ISS.

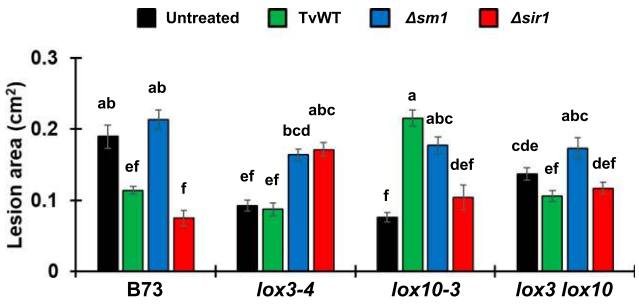

Figure 4. ISR against *C. graminicola* in B73, *lox3-4*, *lox10-3*, and *lox3 lox10* Double Mutant in Response to TvWT, *Δsm1*, and *Δsir1 T. virens* Strain Treatments.

Lesion area caused by *C. graminicola* on the leaves of untreated or TvWT-, *Δsm1*-, or *Δsir1*-treated B73, *lox3-4*, *lox10-3*, or *lox3 lox10* (*lox3-4 lox10-3* double mutant). Infected leaves were scanned and measured using ImageJ software to determine mean lesion area. Bars represent means ± SE of the mean ($n = 5$ maize plants as biological replicates), with letters indicating significant differences among all treatments (Tukey's HSD test, $P < 0.05$). This experiment was repeated at least three times with similar results.

Metabolite Profiling of Xylem Sap Identifies 12-OPDA and KODA as Potential ISR Signals

A previous study revealed that injecting xylem sap from *lox3-4* conferred systemic resistance to B73 receiver plants, thus confirming that xylem sap of the donor *lox3-4* plants contains ISR-relevant signals (Constantino et al., 2013). To determine whether saps from *T. virens*–treated plants were altered in the ability to enhance resistance, we have taken advantage of the sap transfusion methodology developed by Constantino et al. (2013) to circumvent the inability to graft monocots. B73, *lox3-4*, and *lox10-3* plants were left untreated or treated with TvWT, *Δsm1*, or *Δsir1*, and xylem saps were collected at 14 d after treatment. Aliquots of 10 μL of 2× diluted sap were transfused into untreated B73 receiver plants prior to infection with *C. graminicola*. Corroborating the efficacy of the transfusion method, the xylem sap–-treated receiver plants mostly phenocopied the donor plants ISR (Figure 5A). Specifically, the receiver plants treated with sap collected from TvWT-treated B73 or *Δsir1*-treated B73 showed enhanced systemic resistance, as lesions were significantly smaller compared to those that developed on plants treated with sap from untreated B73 or *Δsm1*-treated B73 (Figure 5A). Transfusion with xylem sap from untreated or TvWT-treated *lox3-4* plants also resulted in significantly enhanced resistance, consistent with the findings of Constantino et al. (2013), while sap from *Δsm1*-treated *lox3-4* did not. Transfusion with sap from untreated or *Δsir1*-treated *lox10-3* enhanced resistance, thus mimicking the increased resistance of untreated *lox10* mutant. However, transfusion with the sap from TvWT-treated or *Δsm1*-treated *lox10-3* resulted in increased susceptibility. Interestingly, the sap transfusion results were not restricted to B73, as the sap receiver plants of another inbred line, Tx714, also displayed ISR phenotypes (Figure 5B). These results confirm that the ISR signal(s) are root derived, transported through xylem to aboveground organs to confer systemic resistance, and require functional LOX10. Furthermore, xylem sap from TvWT-treated *lox10-3* conferred ISS to *lox10-3* receiver plants, suggesting that sap from TvWT-treated *lox10-3* contains an as-yet-unknown signal(s) responsible for ISS (Figure 5C). These results suggested that xylem sap from ISR-positive B73 (TvWT- and *Δsir1*-treated plants) and *lox3-4* (untreated and TvWT-treated plants) were enriched with ISR positive signal(s) and therefore were ideal for metabolite profiling in our search for the ISR long-distance signal. These analyses also identified saps lacking ISR activity, which included B73 (untreated and *Δsm1*-treated plants) and *lox3-4* (*Δsm1*- and *Δsir1*-treated plants).

The collected xylem saps were analyzed by liquid chromatography–tandem mass spectrometry (LC-MS/MS) to quantify ~60 diverse oxylipins and several phytohormones, as presented in Supplemental Table 1 and Supplemental Data Set 1. To reduce the number of ISR-relevant candidate metabolites, the following criteria were used for selection of an ISR signal candidate. This molecule(s) had to accumulate at (1) increased levels in the saps from TvWT- and

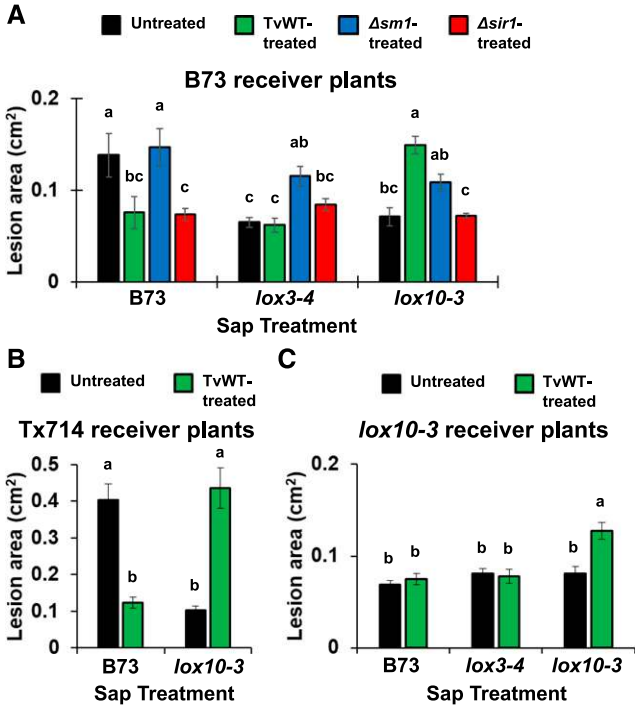

Figure 5. Treatment with Xylem-Derived Sap from the Wild Type and Mutants Treated with *T. virens* Phenocopies the ISR of the Respective Mutants.

(A) Lesion areas caused by *C. graminicola* on B73 receiver plants transfused with xylem sap from untreated or TvWT-, *Δsm1*-, or *Δsir1*-treated B73, *lox3-4*, or *lox10-3* plants.
(B) Lesion areas caused by *C. graminicola* on Tx714 receiver plants after transfusion with xylem sap from untreated or TvWT-treated B73 or *lox10-3* plants.
(C) Lesion areas caused by *C. graminicola* on *lox10-3* (B73 background) receiver plants after transfusion with xylem sap from untreated or TvWT-treated B73, *lox3-4*, or *lox10-3* plants.
Infected leaves were scanned and measured using ImageJ software to determine mean lesion area. Bars represent means ± SE of the mean ($n = 5$ maize plants as biological replicates), with letters indicating significant differences among all treatments (Tukey's HSD test, $P < 0.05$). These experiments were repeated at least two times with similar results.

Δsir1-treated B73 and untreated and TvWT-treated *lox3-4*; (2) reduced levels in the untreated B73, *Δsm1*-treated B73, and *Δsm1*- and *Δsir1*-treated *lox3-4*; and (3) statistically lower levels in *lox10-3* plants regardless of treatment compared with TvWT-treated B73. Of the metabolites and phytohormones detected, only 12-OPDA and KODA, a 9-LOX– and 9-AOS–derived α-ketol (Vick and Zimmerman, 1984; Yokoyama et al., 2000), met all three criteria (Figures 6A to 6C). Specifically, the results showed that these two oxylipins were enriched in the saps with potent ISR activity, which include TvWT- and *Δsir1*-treated B73 and untreated and TvWT-treated *lox3-4* (Figures 6B and 6C). Xylem sap from the plants not displaying ISR, which consisted of untreated B73, *Δsm1*-treated B73, and *Δsm1*- and *Δsir1*-treated *lox3-4*, accumulated 12-OPDA and KODA at much lower levels. Surprisingly, neither JA nor JA-Ile met the three criteria, as their levels did not correlate with the sap ISR activity. Specifically, JA levels were significantly elevated in B73 colonized by *Δsm1* and *Δsir1* (Figure 6D). Interestingly, JA-Ile levels were not elevated in the saps from TvWT-treated B73 and untreated *lox3-4* (Figure 7E), both of which induced strong ISR (Figure 4). Not surprisingly, low levels of 12-OPDA, JA, and JA-Ile were detected in all *lox10-3* plants regardless of treatment (Figure 6), consistent with previous report that *lox10* mutants were unable to accumulate the three jasmonates in wounded leaves (Christensen et al., 2013).

Because traumatic acid synthesis requires functional LOX10 in leaves (Christensen et al., 2013), this molecule was considered a potential ISR signal. However, contents of this molecule were reduced in sap from B73 treated with all *T. virens* strains (Figure 6F). Lastly, SA accumulation levels did not correlate with the ISR phenotypes conferred by the diverse sap samples and were not altered greatly between the different treatments (Figure 6G). These data suggest that of all the known LOX10 products, only 12-OPDA appears to be relevant for ISR. Levels of KODA, a 9-LOX product, appears to be influenced, but not directly produced, by LOX10, which is predominantly a 13-LOX (Nemchenko et al., 2006). Experiments are currently underway to identify which of the six maize 9-LOXs is responsible for the biosynthesis of KODA.

12-OPDA and KODA, but Not JA, Increase Plant Resistance in a Dose-Dependent Manner

To directly test the effect of 12-OPDA and KODA, B73 plants were transfused with different, but biologically relevant, concentrations of 12-OPDA or KODA to identify any effect on maize systemic resistance. To mimic the sap transfusion methods used previously, 12-OPDA or KODA was added to sap from untreated B73 plants and transfused to B73 receiver plants grown without *T. virens*. Positive control treatment for ISR activity was transfusion with the sap from TvWT-treated B73 plants, while negative control treatment was transfusion with the sap from untreated B73. After transfusion, the leaves of treated B73 plants were challenged with *C. graminicola*. Transfusion with the sap supplemented with 12-OPDA enhanced resistance in a dose-dependent manner, with significant reduction of lesion area conferred by 25 nM, 100 nM, and higher 12-OPDA (Figure 7A). Similarly, transfusion with KODA in a similar concentration range also resulted in a dose-dependent effect on enhancing resistance, with the strongest effect occurring between 100 and 1000 nM (Figure 7B).

As 12-OPDA is a reactive electrophilic species (RES), which contain a α,β-unsaturated carbonyl structure and have been shown to activate expression of many defense genes in Arabidopsis and maize (Alméras et al., 2003; Christensen et al., 2015), one possibility is that enhanced maize resistance associated with 12-OPDA transfusion was due to RES activity. In order to differentiate 12-OPDA–specific activity from more general RES activity, B73 were transfused with saps supplemented with equivalent to 12-OPDA range of concentrations of the mammalian hormone prostaglandin A1 (PGA1), a RES not produced in plants (Mueller et al., 2008). None of the concentrations of PGA1 used resulted in enhanced resistance, suggesting that 12-OPDA effect on maize resistance to *C. graminicola* was not due to RES activity (Figure 7C).

While JA-Ile was not an ISR signal candidate from our metabolite profiling of xylem saps, JA-Ile has been implicated in ISR

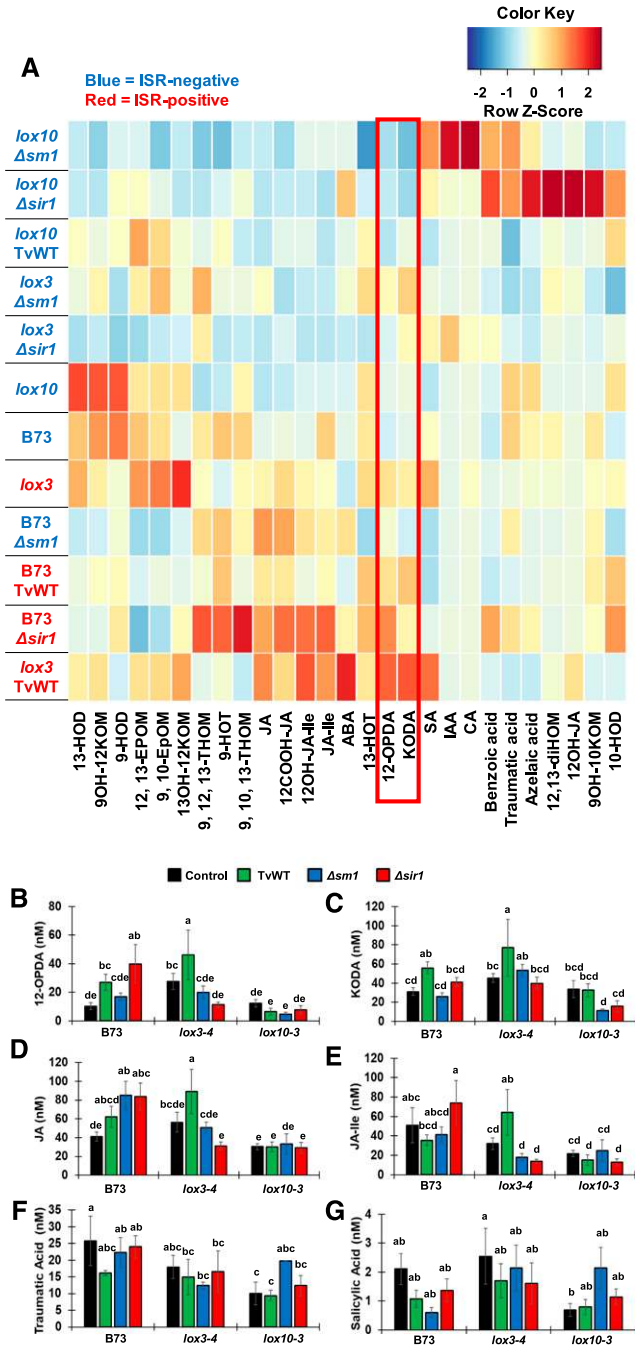

Figure 6. Metabolites and Phytohormones Detected in Xylem Sap from Diverse *T. virens*–Treated Maize.

(A) Heatmap of accumulation of metabolite and phytohormone levels in xylem sap collected from untreated or TvWT-, *Δsm1*-, or *Δsir1*-treated B73, *lox3-4*, or *lox10-3* 14 d after the treatments, represented by Z-score transformed concentrations (number of standard deviations above/below the mean of the column). Combinations of maize and *T. virens* that lack ISR are represented in blue font, while combinations that are positive for ISR are represented in red font. Both 12-OPDA and KODA are boxed as the candidate ISR signals due to higher accumulation in ISR-positive saps and lower accumulation in ISR-negative saps. Full names of measured metabolites and phytohormones are listed in Supplemental Table 1.

(B) to **(G)** Concentrations of **(B)** 12-OPDA, **(C)** KODA, **(D)** JA, **(E)** JA-Ile, **(F)** traumatic acid, and **(G)** SA in xylem sap collected from untreated, TvWT-, *Δsm1*-, or *Δsir1*-treated B73, *lox3-4*, or *lox10-3* plants. Bars represent means ± SE of the mean ($n = 5$ maize plants as biological replicates), with letters indicating significant differences among all treatments (Tukey's HSD test, $P < 0.05$). This experiment was repeated two times with similar results.

regulation in other species. Therefore, we tested JA-Ile as a supplement in the sap transfusion experiments with the same range of concentrations. JA-Ile concentrations from 1 to 100 nM had no impact on lesion area (Figure 7D). Unexpectedly, JA-Ile at 1000 nM led to enhanced susceptibility. Furthermore, transfusion with the JA-Ile precursor, JA, at 1000 nM concentration also increased susceptibility (data not shown). Lastly, while transfusion with 10 nM 12-OPDA or KODA alone had no significant effect on B73 resistance, simultaneous application of both signals at 10 nM concentration resulted in stronger resistance in receiver plants, suggesting an additive or synergistic effect (Figure 7E). Taken together, these results indicate that 12-OPDA and KODA, not JA or JA-Ile, are the oxylipin signals that positively regulate ISR at physiologically relevant nanomolar concentrations.

To test whether ISR deficiency of *Δsm1*-treated B73 can be rescued by exogenous application of 12-OPDA, we supplemented the saps from untreated B73 (no ISR signal) and *Δsm1*-treated B73 (no ISR signal) with 1 μM 12-OPDA. This treatment to both the untreated and *Δsm1*-treated B73 significantly increased resistance to *C. graminicola* (Figures 8A and 8B). These results suggest that 12-OPDA can complement the lack of ISR activity in both ISR-negative saps. To test whether 12-OPDA can reverse the ISS phenotype of TvWT-treated *lox10-3*, sap samples from untreated or TvWT-treated *lox10-3* were supplemented with 12-OPDA and transfused into untreated *lox10-3* or TvWT-treated *lox10-3*. The results showed that 12-OPDA restored TvWT-treated *lox10-3* resistance to levels found in *lox10-3* not colonized by TvWT, as evidenced by significantly decreased lesion area (Figures 8C and 8D). This suggested that TvWT-treated *lox10-3* ISS is due to reduced 12-OPDA.

JA Is Not Required for *T. virens*–Mediated ISR in Maize

The unexpected results from JA-Ile–enriched sap transfusion posed the question of whether JA-Ile was relevant to *T. virens*–triggered ISR in maize. To directly address this question, we utilized the JA-deficient *opr7 opr8* double mutant, which is devoid of JA biosynthesis in every organ tested (Yan et al., 2012). This mutant was treated with TvWT and infected with *C. graminicola*. The untreated *opr7 opr8* mutants were significantly more resistant to anthracnose leaf blight than untreated B73 plants (Figures 9A and 9B). Surprisingly, in response to TvWT colonization, lesion area was further significantly decreased on *opr7 opr8* leaves, indicating that this mutant was still capable of ISR (Figures 9A and 9B). This was in stark contrast to *lox3-4* plants, whose resistance did not benefit further with TvWT treatment (Constantino et al.,

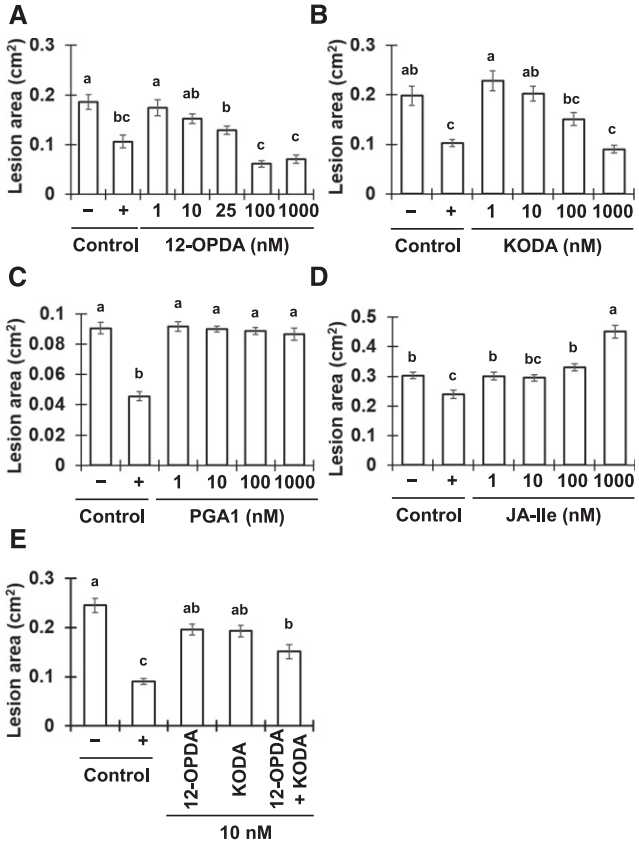

Figure 7. Transfusion with the Sap from Untreated B73 Supplemented with 12-OPDA or KODA Increased Resistance in Receiver Plants in a Dose-Dependent Manner, While Sap Supplemented with JA-Ile Increased Susceptibility.

(A) to **(E)** Lesion area caused by *C. graminicola* on the leaves of B73 plants transfused with saps supplemented with different concentrations of **(A)** 12-OPDA (1, 10, 25, 100, or 1000 nM), **(B)** KODA (1, 10, 100, or 1000 nM), **(C)** PGA1 (1, 10, 100, or 1000 nM), **(D)** JA-Ile (1, 10, 100, or 1000 nM), and **(E)** 12-OPDA and KODA combined (10 nM). Positive control (+) treatment was transfusion with ISR-positive sap from TvWT-treated B73, while negative control (−) treatment was transfusion with ISR-negative sap from untreated B73. Infected leaves were scanned and measured using ImageJ software to determine mean lesion area. Bars represent means ± SE of the mean (n = 5 maize plants as biological replicates), with letters indicating significant differences among all treatments (Tukey's HSD test, $P < 0.05$). These experiments were repeated at least two times with similar results.

2013). These results provide strong genetic evidence that JA is not required for *T. virens*–triggered ISR in maize.

Transcriptomic Analysis Reveals Induction of the Genes Involved in 12-OPDA Biosynthesis or Signaling but Suppression of Downstream JA Biosynthesis and Response Genes

Our findings prompted the hypothesis that JA biosynthesis and 12-OPDA biosynthesis genes may be differentially regulated by *T. virens* colonization. We tested this hypothesis by performing RNA sequencing (RNA-seq) analysis on the roots of B73 seedlings grown in hydroponic conditions and treated with TvWT at 0, 6, and 54 h. The time points represented fungal recognition at 6 h and advanced colonization at 54 h (Malinich et al., 2019). Importantly, the 54-h time point reflects 48 h after the initial 6-h harvest to avoid any transcriptome changes associated with the circadian clock.

In maize, 12-OPDA biosynthesis begins in the plastid with 13-LOXs (LOX7, LOX8, LOX9, LOX10, LOX11, and LOX13) activity, which converts C18:3 to 13(*S*)-hydroperoxylinolenic acid (Figure 10; Borrego and Kolomiets, 2016). As measured by fragments per kilobase of transcript per million mapped reads (FPKM), only *LOX10* expression was induced in response to TvWT recognition, with approximately sixfold increase in transcript abundance compared with untreated plants, consistent with qPCR results (Figure 1A). *LOX7* and *LOX13* transcripts were not detected in any samples. *LOX8* and *LOX9* were expressed only in untreated plants, but they were suppressed by TvWT at both time points. While expression of *LOX11* was unchanged between untreated

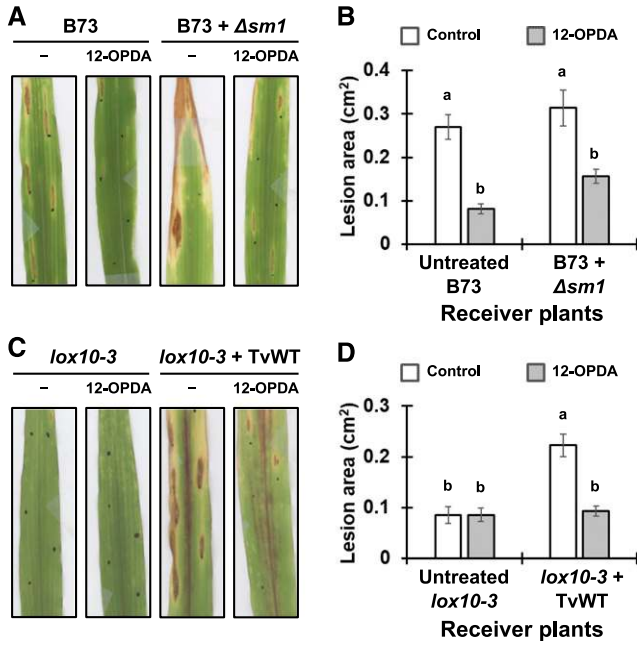

Figure 8. Transfusion with the Sap Supplemented with Exogenous 12-OPDA Enhanced Resistance in B73 and *Δsm1*-Treated B73 and Restored Resistance of TvWT-Treated *lox10-3*.

(A) and **(B)** Visual representation of disease development **(A)** and lesion area **(B)** caused by *C. graminicola* on the leaves of untreated B73 or *Δsm1*-treated B73 receiver plants transfused with the sap from untreated B73 or *Δsm1*-treated B73 donor plants supplemented with 0 (control) or 1000 nM 12-OPDA.

(C) and **(D)** Visual representation of disease development **(C)** and lesion area **(D)** caused by *C. graminicola* on the leaves of untreated *lox10-3* or TvWT-treated *lox10-3* receiver plants transfused with the sap from untreated *lox10-3* or TvWT-treated *lox10-3* donor plants supplemented with 0 nM (control) or 1000 nM 12-OPDA.

Infected leaves were scanned and measured using ImageJ software to determine mean lesion area. Bars represent means ± SE of the mean (n = 5 maize plants as biological replicates), with letters indicating significant differences among all treatments (Tukey's HSD test, $P < 0.05$). This experiment was repeated two times with similar results.

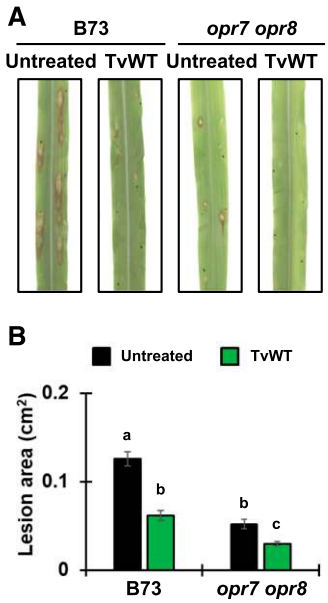

Figure 9. JA Is Dispensable for ISR Induction by *T. virens* Treatment in the JA-Deficient *opr7 opr8* Double Mutant.

(A) and **(B)** Visual representation of disease development **(A)** and lesion area **(B)** caused by *C. graminicola* on the leaves of untreated or TvWT-treated B73 or *opr7 opr8* mutant plants.

Infected leaves were scanned and measured using ImageJ software to determine mean lesion area. Bars represent means ± SE of the mean ($n = 5$ maize plants as biological replicates), with letters indicating significant differences among all treatments (Tukey's HSD test, $P < 0.05$). This experiment was repeated at least three times with similar results.

and TvWT-treated B73 at 6 h, its expression was downregulated at 54 h. These data point to *LOX10* as the sole 13-LOX that was rapidly induced by TvWT even before root colonization took place and support the previous data that *LOX10* is induced by *T. virens* in a Sm1-dependent manner (Figure 1A).

Expression of *AOS1c* and *AOC1*, which encode enzymes involved in conversion of 13(*S*)-hydroperoxylinolenic acid to 12-OPDA, was upregulated at 54 h. Multiple studies have identified genes that are specifically regulated by 12-OPDA, but not by other jasmonates (Taki et al., 2005). Several of these 12-OPDA marker genes were differentially expressed in response to TvWT treatment (Figure 10B). More specifically, a glycosyl hydrolase (*GH9B8*), known to be downregulated in response to 12-OPDA, was repressed after TvWT treatment. On the other hand, expression of several 12-OPDA–upregulated genes, such as Calcium binding EF-hand family protein (*CML41*), zinc finger transcription factor (*ZBF4*), and glutathione transferase (*GST5*), were all significantly increased at 54 h after treatment.

In agreement with the notion that JA is not a major player in ISR induction, expression of both *OPR7* and *OPR8*, the only *OPRs* required for JA biosynthesis (Yan et al., 2012), were downregulated following colonization by TvWT (Figure 10). Furthermore, expression of several genes (*ACX*, *MFP*, and *KAT*) involved in β-oxidation were also downregulated at 54 h. Lastly, among the five *JAR1* maize homologs responsible for the conjugation of Ile to JA (Borrego and Kolomiets, 2016), only *JAR1b* was expressed in the untreated roots, and its transcripts were not detected at 54 h. Taken together, these results suggested that some of the genes responsible for 12-OPDA biosynthesis were upregulated in response to TvWT colonization, but the genes responsible for converting 12-OPDA to JA-Ile were downregulated. qPCR validation of *AOS1c*, *AOC1*, and *OPR7* showed similar trends of expression (Supplemental Figure 2). Our conclusions of induction of 12-OPDA biosynthesis and lack of induction of JA were further corroborated with metabolite profiling of TvWT-treated B73 seedlings roots, which showed significantly increased accumulation of 12-OPDA and KODA at 54 h, but not of JA or JA-Ile (Figures 11A to 11D).

JA-Ile interaction with the COI1-JAZ coreceptor complex results in the degradation of JAZ proteins, negative regulators of JA responses, to allow transcriptional activation of MYC and WRKY transcription factors and induction of JA downstream signaling (Song et al., 2013). Of the six maize *COI1* genes, five genes were expressed in untreated roots, two were rapidly induced at 6 h, and all three were substantially downregulated at 54 h (Figure 10C). Expression of transcription factors *MYC7* and *WRKY46*, implicated in positive regulation of JA-responsive genes (Borrego and Kolomiets, 2016), were repressed at 54 h. Of the *JAZ* genes expressed in roots, *JAZ5*, *JAZ6*, and *JAZ8* transcripts significantly increased at 54 h. Additionally, *CYP94B3B1*, which is involved in JA-Ile catabolism and also known as *tasselseed5* (Lunde et al., 2019), was significantly upregulated by 54 h after TvWT treatment. In agreement with the repression of transcription factors and induction of JA negative regulators, expression of most JA-dependent genes, which include 9-LOX genes (*LOX1* and *LOX5*), OPR genes (*OPR2*, *OPR3*, and *OPR5*), and a phospholipase, *PLC* (Yan et al., 2012), were downregulated at 54 h. Overall, upregulation of several *JAZ* genes, which encode JA-response repressors, and downregulation of JA-dependent genes suggest that *T. virens* colonization results in suppression of JA responses.

In agreement with observed suppression of JA signaling, several SA biosynthesis and signaling genes are significantly upregulated at the time of colonization, likely due to the well-documented SA-JA antagonism (Pieterse et al., 2012). Specifically, expression of all phenylalanine ammonia lyase (*PAL*) genes were strongly upregulated at 54 h, with the exception of *PAL4* (Figure 10D). Similarly, expression of SA-responsive genes, *PR1*, *PR5*, and *PR10*, was significantly upregulated at 54 h as well. qPCR validation of *PR1* and *PR5* expression was in agreement with the RNA-seq results, showing that both transcripts were increased incrementally from 6 to 54 h (Supplemental Figure 2). Surprisingly, expression of *NPR1*, a major component of SAR signaling, was significantly downregulated at 54 h. While the transcriptome data suggest upregulation of SA biosynthesis and downstream signaling, metabolite profiling of TvWT-treated B73 seedlings roots actually showed no significant change in SA levels over the time course (Figure 11E).

DISCUSSION

12-OPDA Is a Mobile Signal for ISR Induction

Multiple long-distance signaling molecules that regulate SAR have been identified (Klessig et al., 2018). By contrast, long-distance

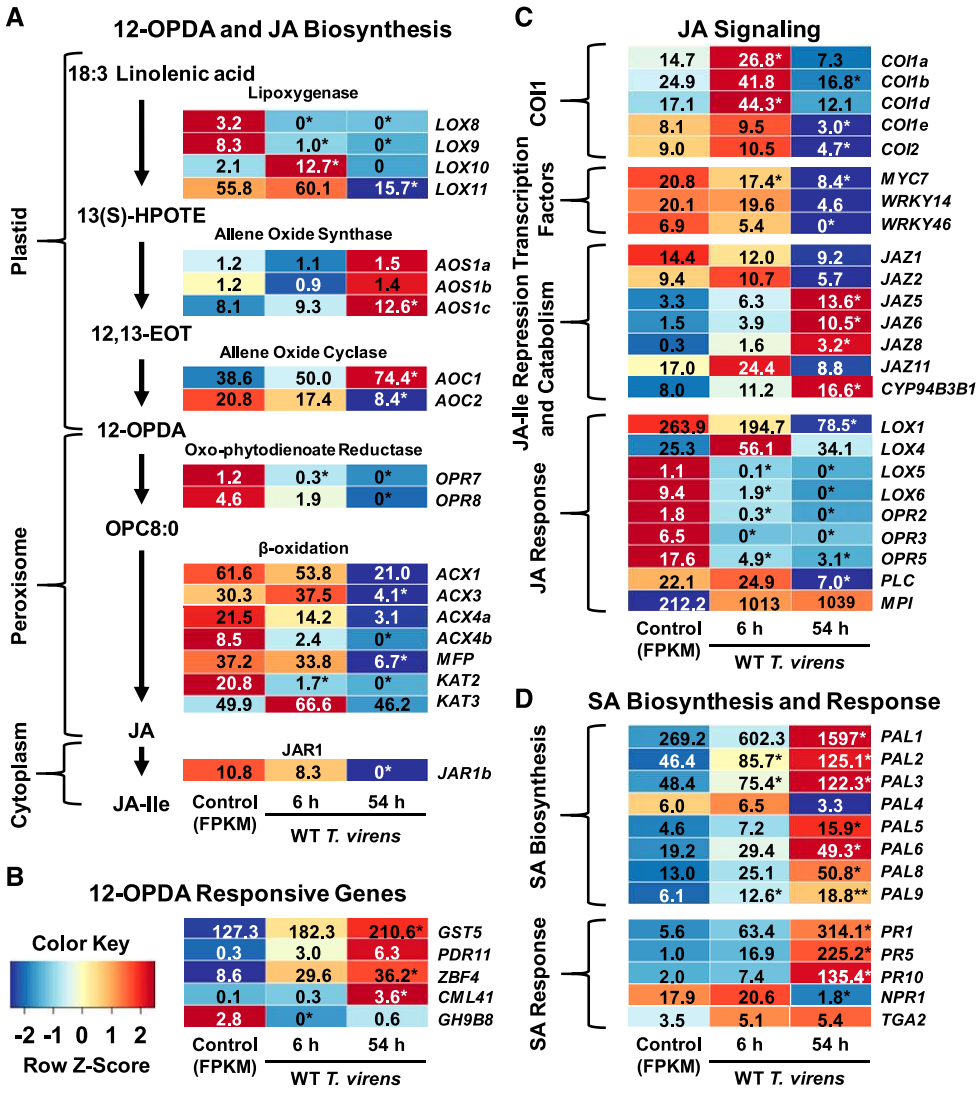

Figure 10. Maize-*T. virens* Interactions Upregulates Genes for 12-OPDA Biosynthesis and Response, but Not Genes Downstream of 12-OPDA for JA or JA-Ile Biosynthesis and Signaling.

(A) to **(D)** Heatmaps of transcript accumulation measured by RNA-seq of **(A)** the AOS pathway branch genes, **(B)** 12-OPDA–responsive genes, **(C)** JA downstream signaling genes, and **(D)** SA biosynthesis and response genes, represented by Z-score–transformed FPKM (number of standard deviations above/below the mean of the row). Values represent average FPKM, with asterisks (*) denoting significant differences compared with untreated plants (Tukey's HSD test, $P < 0.05$). Treatments comprised of untreated B73 plants ($n = 4$), and TvWT-treated plants ($n = 10$) at 6 and 54 h. Gene IDs and functions of each gene are listed in Supplemental Table 2. *n* is the number of biological replicates consisting of plants grown in hydroponic jars, each consisting of five maize seedlings.

signals responsible for establishing ISR remain less characterized, with most studies pointing to JA and ethylene as the two signaling pathways involved (Pieterse et al., 2014b). In this study, we utilized genetic, biochemical, and pharmacological approaches with ISR-positive and -negative mutants of both *T. virens* (*Δsm1* and *Δsir1*) and maize (*lox3* and *lox10*) to identify the JA precursor 12-OPDA as a major signal responsible for regulating *T. virens*–triggered ISR in maize. The *lox10* mutants, reduced in 12-OPDA content (Christensen et al., 2013), not only lost the capacity for *T. virens*–induced ISR against both hemibiotrophic and necrotrophic pathogens but also displayed ISS in response to TvWT treatment (Figures 2 and 3). Importantly, 12-OPDA transfusion restored ISR in TvWT-treated *lox10-3* to the levels observed with TvWT-treated B73 plants (Figure 8), indicating that 12-OPDA deficiency contributed to the lack of ISR in *lox10* mutants. Furthermore, 12-OPDA levels in xylem sap were higher in plants that displayed ISR and lower in those that did not (Figures 6A and 6B). Transfusion with xylem sap supplemented with low doses of 12-OPDA conferred robust ISR phenotype, with increasing concentrations of 12-OPDA resulting in stronger systemic resistance against *C. graminicola* (Figure 7A). The dose-dependent effect of 12-OPDA in triggering maize systemic resistance is a characteristic property of a hormone. This enhanced

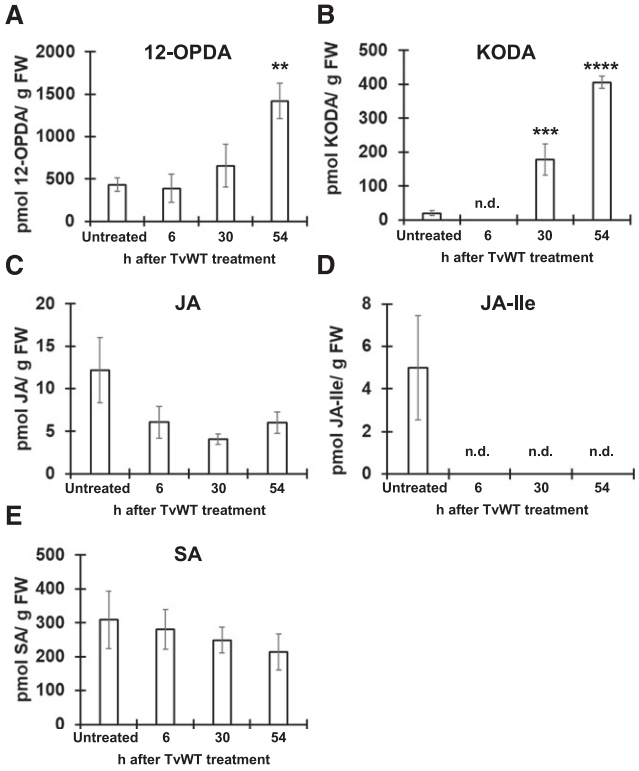

Figure 11. Metabolite Profiling of TvWT-Treated Maize Seedling Roots Reveal Increased Accumulation of 12-OPDA and KODA.

(A) to **(E)** Accumulation of **(A)** 12-OPDA, **(B)** KODA, **(C)** JA, **(D)** JA-Ile, and **(E)** SA in the root tissues of untreated or TvWT-treated B73 seedlings grown under hydroponic conditions at 6, 30, and 54 h after TvWT treatment. Bars represent means ± SE of the mean ($n = 5$ biological replicates of plants grown in hydroponic jars, each consisting of five maize seedlings). Statistical significance was determined with Tukey's HSD test (*$P < 0.05$, **$P < 0.01$, ***$P < 0.001$, ****$P < 0.0001$).

resistance was not due to RES activity and was 12-OPDA specific, as transfusion with PGA1 had no effect on resistance against infection (Figure 7C). This was further supported by the lack of induction of RES-response marker genes, such as *GST25* (*Zm00001d048558*), *TolB* (*Zm00001d022277*), and *CYP81D11* (*Zm00001d030856*), in response to TvWT treatment (Supplemental Figure 3). One interesting observation is that despite the low levels of 12-OPDA, the untreated *lox10* mutants were significantly more resistant compared with untreated B73 (Figures 2 and 3).

These results raise the question of how previous research did not identify 12-OPDA as an ISR signal. While 12-OPDA is a precursor of JA, there is growing evidence that the signaling functions of 12-OPDA are vastly different from those of JA (Dave and Graham, 2012; Christensen et al., 2015; Maynard et al., 2018). Microarray analysis of Arabidopsis treated with 12-OPDA, JA, or methyl-JA revealed a set of genes that responded only to 12-OPDA in a COI1-independent manner (Taki et al., 2005; Mueller et al., 2008). Recent studies revealed that there exists OPDA-Ile conjugate, lending credence to 12-OPDA being an independent signal in the same manner as JA (Floková et al., 2016). A recent maize study revealed that resistance to aphids (*Rhopalosiphum maidis*) is mediated by 12-OPDA, while JA-Ile was not required for defense against these sucking insects (Varsani et al., 2019). Additionally, Arabidopsis resistance to root-knot nematodes (*Meloidogyne hapla*) was reliant on the accumulation of 12-OPDA, not JA, as mutants deficient in the production of 12-OPDA and JA were hyper-susceptible, but mutants deficient in JA only were as resistant as the wild-type plants (Gleason et al., 2016). *OPR3*-silenced tomato mutants showed dramatically lower levels of 12-OPDA and downstream JA products; however, treatment with 12-OPDA, not JA, had a significant effect in restoring plant basal resistance against *Botrytis cinerea* (Scalschi et al., 2015). In *AOC* overexpressor lines of rice (*Oryza sativa*), higher accumulation of 12-OPDA led to increased resistance against brown planthoppers (*Nilaparvata lugens*), a piercing-sucking insect (Guo et al., 2014). Additionally, treatment with 12-OPDA, but not JA or JA-Ile, led to enhanced resistance against the planthoppers in rice. Supporting our findings, tomato JA-deficient mutant *def1* lost the capacity for ISR against *Fusarium* infection when treated with *T. virens* (Jogaiah et al., 2018). While the authors assigned the lack of ISR to loss of JA in *def1*, they did not examine whether 12-OPDA may have been responsible for the loss of ISR, as the mutant was determined to be disrupted in both 12-OPDA and JA biosynthesis (Howe et al., 1996). Increase in 12-OPDA, but not JA, content also correlated with tendril coiling in *Bryonia dioica* (Stelmach et al., 1998; Blechert et al., 1999).

Interestingly, the liverwort *Marchantia polymorpha* accumulated 12-OPDA in response to wounding, but it was unable to produce JA (Yamamoto et al., 2015). Similarly, the moss *Physcomitrella patens* lacks the enzymes that convert 12-OPDA to JA, but it still maintained the components for JA perception and signaling (Stumpe et al., 2010; Ponce De León et al., 2012). Furthermore, a recent study found that *M. polymorpha* COI1 was functionally conserved with AtCOI1 but recognized dinor-OPDA as a ligand rather than JA-Ile (Monte et al., 2018). A single amino acid substitution between MpCOI1 and AtCOI1 was responsible for the switch in ligand specificity, suggesting that 12-OPDA is the more ancient jasmonate signal and that JA-Ile arose later. These revelations on COI1 also raise the possibility that, unlike the single COI1 in Arabidopsis, some of the six distinct COI1 proteins of maize, especially COI2, which is unable to complement a *coi1* mutant of Arabidopsis (An et al., 2018), may perceive 12-OPDA rather than JA-Ile.

A possible explanation for why 12-OPDA is overlooked is that most research has focused specifically on JA. Since JA downstream signaling also results in a positive feedback loop for JA biosynthesis (Wasternack, 2007), JA-insensitive mutants would lack that positive feedback and be unable to trigger upregulation of both JA and 12-OPDA biosynthesis. Tomato *spr2*, the mutant in a fatty acid desaturase, is impaired in wound-induced JA biosynthesis due to more than 90% decreased C18:3 content in leaves (Li et al., 2003), and it is unable to establish mycorrhiza-induced resistance (Song et al., 2015). It was not reported whether this mutant also lacked 12-OPDA in roots, although 12-OPDA levels were significantly reduced in seeds (Goetz et al., 2012).

Furthermore, treating cucumber (*Cucumis sativus*) roots with the 12-OPDA and JA biosynthesis inhibitor diethyldithiocarbamic acid (Farmer et al., 1994), blocked *Trichoderma asperellum*–-triggered ISR (Shoresh et al., 2005). In both cases, the focus of the

studies was on the end product, JA, and not the intermediaries such as 12-OPDA.

9-Oxylipin KODA Is a Novel Candidate Long-Distance ISR Signal

Another key finding of this study is the identification of KODA as another potential ISR signal. While accumulation of KODA, a 9-LOX and 9-AOS pathway product (Yokoyama et al., 2000; Howe and Schilmiller, 2002; Sakamoto et al., 2010), in xylem sap may be affected by LOX10 function, LOX10 is a 13-LOX (Nemchenko et al., 2006) and therefore is not likely to be responsible for KODA production. The function of KODA has been studied only rudimentarily, with several reports indicating that KODA has flowering-promotion effects in duckweed (*Lemna paucicostata*), apple (*Malus domestica*) trees, and Japanese pear (*Pyrus pyrifolia*; Yokoyama et al., 2000; Kittikorn et al., 2010; Sakamoto et al., 2010). KODA was also reported to accumulate at high levels in duckweed after exposure to abiotic stresses such as drought, heat, or osmotic stresses (Yokoyama et al., 2000). Wheat treated with KODA displayed enhanced abiotic stress tolerance by promoting root elongation, increased germination rate and seedling growth, and improved drought tolerance (Haque et al., 2016). One study demonstrated that exogenous application of KODA enhanced grape resistance against *Glomerella cingulata* and induced high levels of *LOX* and *AOS* expression (Wang et al., 2016), which may suggest that KODA induced 12-OPDA biosynthesis. Interestingly, application of KODA had no impact on pathogen growth on agar media, suggesting that KODA had no antimicrobial properties (Wang et al., 2016). This is in stark contrast to 12-OPDA, which has been reported to inhibit growth of several fungal pathogens (Prost et al., 2005). This brings up the question of whether sap-transfused 12-OPDA in this study may have direct antifungal activity against *C. graminicola* in leaves. However, the concentration used in the Prost et al. (2005) study was 100 μM, a concentration 100 times higher than the highest concentration of 1 μM used in this study. Additionally, while we did observe higher levels of 12-OPDA and KODA in B73 roots in response to TvWT treatment, levels of both metabolites in shoot tissue were not significantly altered (Supplemental Figure 4). It is equally unlikely that sap-transfused 12-OPDA had direct antifungal activity, since untreated *lox10* contained significantly lower levels of 12-OPDA in the leaves (Christensen et al., 2013), yet was significantly more resistant to infection (Figures 2 and 3). While JA and 12-OPDA have been reported to inhibit root growth, it is possible that increased KODA production in response to *T. virens* may be behind simultaneous *T. virens*–promoted growth promotion and ISR induction. Efforts are currently being taken to screen the available 9-LOX maize mutants to identify which is responsible for KODA production.

Is JA a Long-Distance Signal for ISR?

JA signaling is well established as essential for ISR in the *Pseudomonas fluorescens* WCS417r-triggered ISR in Arabidopsis Columbia 0 (Col-0), as the *jar1* mutant lacked the ISR response against *Pseudomonas syringae* pv *tomato* (*Pst*; Pieterse et al., 1998, 2014b). Surprisingly, our study showed that JA and JA-Ile levels in xylem sap did not correlate with the ISR expression in diverse maize–*T. virens* genotype combinations (Figure 6). Rather, transfusion with sap supplemented with JA-Ile resulted in enhanced susceptibility (Figure 7D). Importantly, the analysis of ISR competency of the JA-deficient mutant *opr7 opr8* (Yan et al., 2012) showed that they were capable of mounting ISR (Figure 9A). Moreover, transcriptome analysis of TvWT-treated B73 plants showed upregulation of plastid-localized 12-OPDA biosynthesis genes (*LOX10*, *AOS1c*, and *AOC1*) and several 12-OPDA–specific marker genes but downregulation of JA biosynthesis genes downstream of 12-OPDA (*OPR7*, *OPR8*, β-oxidation genes, and *JAR1*) during colonization (Figure 10). Several JA-Ile repressor or catabolism genes, which include *JAZ* genes and *CYP94B1* (Lunde et al., 2019), respectively, were significantly upregulated, indicating suppression of JA signaling upon TvWT colonization. In support of the transcriptional changes, metabolite profiling of TvWT-treated B73 roots showed increased 12-OPDA and KODA and either low or undetected levels of JA and JA-Ile (Figure 11). Taken together, these results implicate 12-OPDA and KODA, not JA, as the mobile ISR signals in maize. In support of JA being dispensable for ISR, the MiSSP7 effector-mediated suppression of JA was shown to be essential for forming symbiosis between the ectomycorrhizal fungus *Laccaria bicolor* and poplar trees (*Populus* sp; Plett et al., 2011). This effector was shown to stabilize poplar JAZ6 protein, thus repressing JA signaling and allowing for better root colonization (Plett et al., 2014). Similarly, interactions between gray poplar (*Populus canescens*) and the ectomycorrhizal fungus *Paxillus involutus* were reported to increase SA and decrease JA in the roots (Luo et al., 2009).

It is possible that JA was not necessary for *T. virens*–triggered ISR in maize but may be required for interactions between other plant hosts and beneficial microbes. While *P. fluorescens* strain WCS417r-triggered ISR in Arabidopsis Col-0 against *Pst* infection (Pieterse et al., 1998), *P. fluorescens* strain CHA0r could not (Iavicoli et al., 2003). Instead, CHA0r-triggered ISR protected Col-0 against *Peronospora parasitica* infection, but it could not protect the Wassilewskija (Ws)-0 ecotype against the same pathogen. Similarly, *T. harzianum*–triggered ISR in Col-0, but not in the other ecotypes such as Landsberg erecta, Ws-4, or Nossen (Korolev et al., 2008). Furthermore, while the bacterium *Paenibacillus alvei* K165 conferred systemic resistance to Arabidopsis against *Verticillium dahliae* infection, it did not rely on JA signaling, as the *jar1* mutant retained ISR (Tjamos et al., 2005). Rather, *eds5*/*sid1* and *sid2* mutants lost ISR when treated with K165, suggesting that SA played a prominent role in this system. Another example of the complexity of ISR signaling is the study showing the beneficial fungus *Penicillium viridicatum* was able to trigger ISR in both *jar1-1* and *npr1-1* mutants against *Pst* infection (Hossain et al., 2017). While these studies do not address the role of 12-OPDA or KODA, they strongly suggest that there is no consensus ISR signaling pathway and that ISR arises based on specific plant host, beneficial microbe, and pathogen combinations.

SA Roles in Maize–*T. virens* Interactions

Our data showed that while SA biosynthesis and responsive genes were strongly upregulated in response to TvWT colonization

(Figure 10), SA levels in TvWT-treated B73 roots remained unchanged over time (Figure 11E). This may indicate that there exists a fine-tuned balance in the regulation of this defense hormone to accommodate symbiotic interactions. This balance may be regulated not only by the host but also by the beneficial microbes. For example, a study has shown that induction of SA-mediated defenses is necessary to limit *Trichoderma* colonization of roots to the apoplast and exclude colonization of the vascular tissue (Alonso-Ramírez et al., 2014). When colonized by *T. harzianum*, the Arabidopsis SA-induction-deficient mutant *sid2* displayed stunted growth and root rot, and *T. harzianum* was able to spread systemically through the vascular tissue and into the leaves. Additionally, several *Trichoderma* species were shown to degrade SA (Navarro-Meléndez and Heil, 2014; Martínez-Medina et al., 2017; Jogaiah et al., 2018). Our data do not clarify whether SA is required for *T. virens*–triggered ISR in maize, as we did not observe SA increase in xylem sap samples from TvWT-treated plants (Figure 6G) or in the roots (Figure 11E). Interestingly, while SA levels in roots were not altered by TvWT colonization, SA levels in shoot did increase at 54 h (Supplemental Figure 4E). Recently, several salicylate monooxygenase/hydroxylase genes, which degrade SA, were identified in *T. virens* as differentially expressed genes in the presence of maize (Malinich et al., 2019). Therefore, it is possible that *T. virens* may use these enzymes to prevent elevation of host SA levels during colonization of roots. SA-deficient plants will be required to establish the function of SA in ISR.

T. virens Does Not Produce 12-OPDA, KODA, or JA Itself, but Uses Peptide Signals to Differentially Regulate Host Oxylipin Synthesis for ISR

As reported in this study, *LOX10* transcriptional activation as early as 3 to 6 h during interaction between maize roots and *T. virens* required functional fungal peptide signal Sm1 (Figure 1A). Such early activation is consistent with a previous report showing Sm1 is constitutively expressed and secreted continuously by fungal hyphae even in the absence of a host (Djonović et al., 2006). Here, we provided additional evidence that Sm1 is a major peptide signal for ISR by demonstrating that the enhanced ISR activation by *Δsir1* mutant is likely due to a threefold greater expression of *SM1* (Figure 1C). The antagonistic interactions between Sm1 and Sir1 indicate that these peptides may be responsible for different aspects of regulating maize–fungal symbiosis, although the exact mode of action on plant cells by Sm1 or Sir1 remains to be explored.

We had also considered the possibility that *T. virens* may itself be producing the 12-OPDA or KODA that we detected in xylem sap. There is a precedent for plant-associated microbes producing oxylipins such as 12-OPDA and JA. The plant pathogenic fungi *Lasiodiplodia theobromae* (Tsukada et al., 2010) and *Fusarium oxysporum f*. sp *tulipae* (Oliw and Hamberg, 2017) were shown to produce 12-OPDA and other jasmonates. Additionally, several endophytic bacteria isolated from sunflowers (*Helianthus annuus*) produce 12-OPDA and JA in growth media and under drought conditions (Forchetti et al., 2007). With regard to *T. virens*, however, we were unable to detect any discernable chromatograph signals for 12-OPDA, KODA, or JA within the fungus or in the surrounding media.

Does the Balance between TvWT-Induced Growth Promotion and ISR Involve Differential Regulation of 12-OPDA and JA?

In the field of symbiont–host interactions, one of the mysteries that remains to be explored is the mechanism by which beneficial microbes induce ISR defense and promote plant growth simultaneously. Plant growth and defense trade-offs can occur depending on environmental cues, prompting the plant to devote more resources toward defense responses or toward growth in the absence of stresses (Huot et al., 2014). There is overwhelming evidence that increased JA can result in impaired plant growth (Wasternack and Hause, 2013; Huang et al., 2017; Dubois et al., 2018). Exogenous JA treatment results in reduced root growth, leaf expansion, and hypocotyl growth in Arabidopsis (Wasternack and Hause, 2013). Most recently, overexpression of a plastid lipase gene was shown to result in significantly higher accumulation of JA, reducing vegetative growth even when Arabidopsis was grown in nutrient-rich media (Wang et al., 2018).

In maize, improper balancing between plant growth and defense could be best observed with *lox3* mutants, which overproduce defense hormones SA, JA, and ethylene in the roots and display constitutive ISR, but have reduced germination rate, reduced height by ~25 to 30%, and prematurely senesce (Gao et al., 2008). If JA is a major signal for ISR induction by beneficial microorganisms, but inhibits growth, then it remains unclear how the symbionts could also promote plant growth. The identification of 12-OPDA and KODA, rather than JA, as ISR signals provides an intriguing venue to explore how this widely reported growth-defense balance by *T. virens* is achieved. Currently, studies on the effect of 12-OPDA on plant growth suggest an inhibitory role similar to that of JA, although the concentrations used in those studies may not have been biologically relevant (25 and 50 μM; Yamamoto et al., 2015). While 12-OPDA was shown to promote Arabidopsis (Col-0 and Ws backgrounds) seed dormancy, Yamamoto et al. (2015) and Dave et al. (2011) used much higher concentrations (10 and 50 μM) in the growth media. Our results showed that despite triggering ISS and over-colonizing *lox10* roots (Supplemental Figure 1A), *T. virens* had no detrimental effect on *lox10* plant biomass (Supplemental Figures 1B and 1C). The different levels of 12-OPDA between B73 and *lox10-3* mutant plants did not correlate with plant growth, suggesting that growth promotion and ISR are distinct pathways. Supporting this notion is the previous report showing that *T. harzianum* was able to enhance growth of Arabidopsis mutants that were unable to mount ISR (Korolev et al., 2008).

Working Model of Oxylipin Regulation of ISR Response

A summary of the maize ISR process induced by *T. virens* is presented in the working model presented in Figure 12. In short, *T. virens* root colonization results in the suppression of the negative regulator of ISR, *LOX3*, in a Sm1-dependent manner (Constantino et al., 2013), which allows the upregulation of *LOX10* (Gao et al., 2008; Constantino et al., 2013). Upregulation of *LOX10* and the 12-OPDA biosynthesis genes (*AOS1c* and *AOC1*) results in increased accumulation of 12-OPDA. Simultaneously, JA biosynthesis and signaling are downregulated, which may help accommodate root

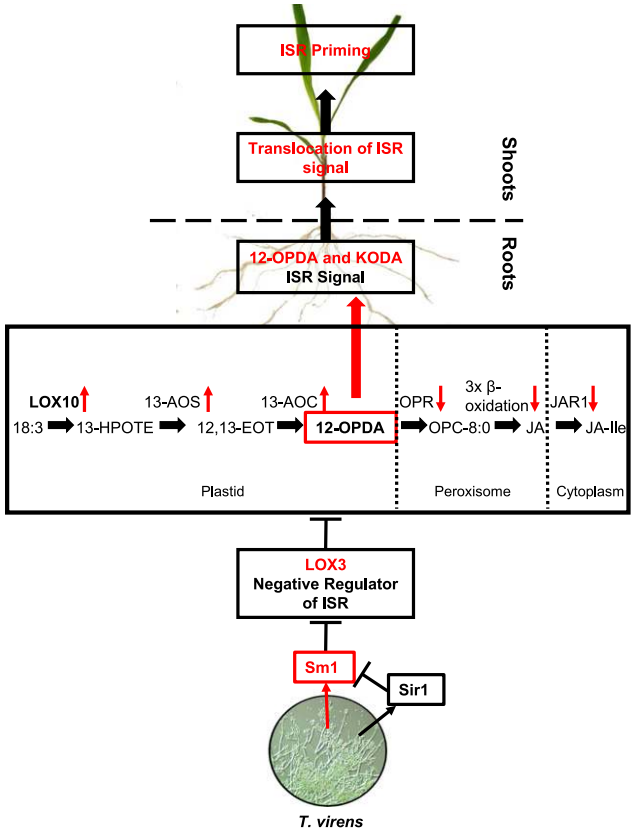

Figure 12. Model of *T. virens*–Triggered ISR in Maize.

The below-ground interactions between maize roots and *T. virens* result in the transcriptional and metabolic reprogramming of the roots that lead to synthesis of a long-distance ISR signal(s) that travels systemically within the xylem to confer resistance throughout the plant against a broad range of pathogen infection. *T. virens* produces the small peptides Sm1, which promotes ISR, and Sir1, which suppresses expression of *SM1*, resulting in suppression of ISR. The fungus suppresses *LOX3* and induces *LOX10* expression, either sequentially or concurrently, in a Sm1-dependent manner. The ISR signals, 12-OPDA and KODA, are able to significantly improve systemic resistance and rescue susceptibility.

colonization by *T. virens*. It is possible that increased 12-OPDA leads to increased biosynthesis of yet additional mobile signal, KODA, produced in the 9-LOX/9-AOS branch of the LOX pathway. Both 12-OPDA and KODA are transported through xylem to confer systemic resistance throughout the rest of the plant.

METHODS

Plant and Fungal Material

The maize (*Zea mays*) inbred lines B73, W438, and Tx714 and mutator transposon knockout mutants *lox3-4* (Gao et al., 2007), *lox10-2*, *lox10-3* (Christensen, 2009), and double mutant *opr7 opr8* (*opr7-5 opr8-2*; Yan et al., 2012) were used in this study. The mutant maize lines are all near-isogenic at the BC_7 genetic stage in the B73 or W438 genetic backgrounds. The double mutant *lox3 lox10* was generated by crossing single mutants *lox3-4* and *lox10-3* at the BC_7 stage and identified from the segregating populations of BC_7F2 by using PCR primers as described previously by Gao et al. (2007) and Christensen et al. (2013).

Strains Gv29-8 (TvWT; Baek and Kenerley, 1998), *Δsm1* (Djonović et al., 2006), and *Δsir1* (formerly *Δ77560*; Lamdan et al., 2015) of *Trichoderma virens* were grown on Potato Dextrose Agar (catalog no. 213200, BD Difco Laboratories) at 27°C from glycerol stock cultures maintained at −80°C. Chlamydospores of *T. virens* were obtained from cultures grown in molasses-yeast extract medium (Mukherjee and Kenerley, 2010). After 2 weeks, the incubated cultures were vacuum filtered and air dried, and the mycelial mat containing chlamydospores was ground to fine powder. *Colletotrichum graminicola* (1.001 strain) on Potato Dextrose Agar and *Cochliobolus heterostrophus* on complete medium with Xyl (substituted for Glc to improve conidiation) were grown at room temperature (21 to 23°C) under fluorescent lights (Tzeng et al., 1992).

Soil Growth Conditions

Maize seeds were surface sterilized with 70% (v/v) ethanol for 5 min, followed with a 0.6% (v/v) sodium hypochlorite wash for 5 min, and then rinsed three to five times with sterile water. The seeds were planted in sterilized (steam sterilized for 1 h, cooled overnight, and sterilized again for 1 h) soil (MetroMix 360 Rsi, Sun Gro Horticulture) in long cone-tainers (catalog no. SC10R, Stuewe and Sons). The plants were grown on light shelves at room temperature (21 to 23°C) under three 6500K blue and three 3000K red fluorescent lights (catalog nos. 901618 and 901619, respectively; Spectralux) with a 14-h light period.

ISR Assay

Infection with C. *graminicola* and *C. heterostrophus* was performed in this study as described by Gao et al. (2007). Seven days after maize seeds were planted, similarly developed seedlings were either left untreated or treated with 0.1 g of *T. virens* chlamydospores (added to the soil at a depth of 4 to 5 cm). When the plants reached vegetative stage 4, the third true leaves were infected with *C. graminicola* or *C. heterostrophus*. Briefly, the plants were placed in trays (78.5 × 63 × 7 cm) lined with paper towels with the third leaves taped down flat. To harvest spores, 5 mL of sterile water was added to *C. graminicola* or *C. heterostrophus* plates that were then scraped with an inoculating loop to free the conidia. The suspension was filtered through sterile cheesecloth into a 50-mL Falcon tube to remove mycelia. The conidial suspension was centrifuged twice at 3000 rpm for 3 min, with the water being replaced each time with fresh sterile water. The initial conidia concentration was determined using a hemocytometer. The suspension was finally diluted to a concentration of 10^6 spores/mL. Ten microliters of the spore suspension (10,000 spores) was drop inoculated to six individual areas of the middle part of the leaf on both sides of the midvein. Paper towels were moistened with sterile water and were then covered with plastic wrap (GLAD Press'n'Seal) to create a humid chamber. The humidity chambers were placed in darkness for 24 h at 25°C. The plants were then positioned upright and returned to light shelves. Leaves were scanned 4 d after infection, and lesion area was determined using the ImageJ software (https://imagej.nih.gov/ij/).

Root Colonization Assay

Surface-sterilized maize seeds were germinated on Luria-Bertani (LB; catalog no. 244510, BD Difco Laboratories) agar plates for 3 d and then transplanted 2.5 cm deep into sterile, capped test tubes with 30 g of sterile soil (2:3 ratio of sand to loam) mixed with sterile water (ratio, 1 mL/10 g of soil) and *T. virens* chlamydospores (0.03 g chlamydospore/1 g of soil) with a hand mixer for 1 min. After 7 d, the plants were gently removed from the test tubes, and soil was gently rinsed off the roots. The roots were washed by submerging in 1% (w/v) sodium metaphosphate solution and shaking at

50 rpm for 30 min. The roots were subsequently washed with sterile water at 50 rpm for 30 min and then surface sterilized by submerging in 1% (v/v) bleach and shaking at 50 rpm for 1 min. The roots were washed with sterile water until the bleach smell was removed. The sterilized roots were measured for total biomass, cut into small pieces, and laid flat on *Trichoderma*-selective GVSM media (Park et al., 1992). After 48-h incubation at 27°C, colony-forming units emerging from the roots were counted. Root colonization data are expressed as colonies per gram of root weight.

Xylem-Enriched Sap Collection

Xylem-enriched sap was collected from B73, *lox3-4*, and *lox10-3* plants treated with the wild type, *Δsm1*, or *Δsir1* strains of *T. virens* or left untreated as described above. Seven days after maize seeds were planted, similarly developed seedlings were either left untreated or treated with 0.1 g of *T. virens* chlamydospores and placed on the growth shelves as described above. After 14 d when the plants reached vegetative stage 4, the plants were kept well saturated with water (Constantino et al., 2013). The plants were then decapitated by a diagonal cut with a scalpel above the first leaf. The first droplet of sap was discarded to avoid collecting wounding-related signals. The droplets after that were collected for 3 h and stored on ice. The plants were also periodically recut when sap flow declined, with the first new droplet being discarded. The saps were spun down to remove debris, and the final sap collections were stored in −80°C until needed for the experiments.

Xylem Sap Transfusion Assay

Collected xylem-enriched saps were transfused into a small cut along the pseudo-stem of receiver plants as described by Constantino et al. (2013). In short, to perform sap transfusion, receiver plants were placed on their sides in trays lined with paper towels with the third true leaves taped down flat as previously described by Constantino et al. (2013). One incision was made with a scalpel between the first and second leaves, and 10 μL of water or xylem sap diluted 1:1 with water was added into each incision. For transfusion assays with saps supplemented with 12-OPDA (catalog no. 88520, Cayman Chemical), KODA (catalog no. 13-1828, Larodan AB), PGA1 (catalog no. 10010, Cayman Chemical), or JA-Ile (catalog no. 10740, Cayman Chemical), the protocol for xylem sap transfusion assay was slightly modified. Xylem sap from untreated B73 was diluted 1:1 with water for control or different concentrations of the metabolites. Three hours after sap transfusion, plant leaves were drop inoculated with *C. graminicola* as described above.

Quantification of Xylem Sap Metabolites

Xylem-enriched sap and fresh maize tissue metabolites were quantified using LC-MS/MS. For analysis of metabolites in xylem-enriched sap samples, 90 μL of a 1:1 diluted sap solution was mixed with 10 μL of 5 μM isotopically labeled internal standards [d-ABA ([2 H6](+)-*cis*,*trans*-abscisic acid, OlChemIm), d-IAA ([2 H5]indole-3-acetic acid, OlChemIm), d-JA (2,4,4-d3; acetyl-2,2-d2 JA, CDN Isotopes), and d-SA (d6-SA, Sigma-Aldrich)]. For analysis of metabolites in fresh tissue, 100 mg of root tissue was finely ground under liquid nitrogen and mixed with 500 μL of phytohormone extraction buffer (1-propanol/water/HCl [2:1:0.002 v/v/v]) containing 5 μM of the isotopically labeled internal standards listed above. The samples were agitated for 30 min at 4°C, and 500 μL of dichloromethane was added to each sample. The samples were agitated again for 30 min at 4°C and then centrifuged at 14,000*g* for 5 min. The lower layer of each sample was transferred to a glass vial for evaporation under a nitrogen gas stream. The samples were resuspended in 150 μL of methanol, transferred to a 1.5-mL microcentrifuge tube, and centrifuged at 14,000*g* for 2 min to pellet any debris. Supernatant (90 μL) of each sample was transferred into autosampler vials with glass inserts. For both sample-types, a 15-μL aliquot was injected into an API 3200 LC-MS/MS system (Sciex) using electrospray ionization in negative mode with multiple reaction mentoring. After integration with Analyst v1.6.3 (Sciex), the concentrations of endogenous metabolites were determined by comparing peak areas against isotopically labeled internal standards using appropriate response factors. The chromatography was performed with an Ascentis Express C-18 column (3 cm × 2.1 mm, 2.7 μm; Sigma-Aldrich). The mobile phase was set at 400 mL/min consisting of solution A (0.02% [v/v] acetic acid in water) and solution B (0.02% acetic acid in acetonitrile) with a gradient consisting of the following (time in minutes – % [v/v] solution B): 0.5 – 10%, 1.0 – 20%, 21.0 – 70%, 24.6 – 100%, 24.8 – 10%, 29 – stop. All hormones and oxylipins were quantified by comparing levels of endogenous metabolites to isotopically labeled standards from Sigma-Aldrich, Cayman Chemical, and Larodan AB, with appropriate response factors (Müller and Munné-Bosch, 2011; Christensen et al., 2014). The metabolite and phytohormone *m/z* values and retention times are listed in Supplemental Table 1.

Hydroponic Growth Conditions for RNA-Seq

To study the effects of colonization by *T. virens* on maize root transcriptome, a hydroponic system as described by Djonovic et al. (2007) was used to prevent contamination and minimize mechanical damage. Maize seeds were surface sterilized with a 70% (v/v) ethanol wash for 5 min, rinsed with sterile water, washed with 10% (v/v) hydrogen peroxide for 2 h, and finally rinsed with sterile water. The seeds were plated on LB agar plates and incubated at 28°C in humidity chambers. The seeds were checked every day for signs of bacterial or fungal contamination, and clean seeds were carefully transferred to fresh LB plates. After 7 d, clean and uniformly germinated seeds were selected and placed in hydroponic jars consisting of a Ball wide mouth canning jar (16 oz) with a 125-mL shaker clamp (catalog no. EW-51706-78, Thermo Fisher Scientific) supporting a plastic mesh stage, and filled with 200 mL of half-strength Murashige and Skoog (MS) media with Gamborg vitamins (catalog no. M0404, Sigma-Aldrich) at pH 5.6. Each jar contained five seedlings positioned so that the tap roots threaded through the mesh and were in contact with the MS media. The jars were capped with the bottom of sterile plastic Petri plates (100 × 15 mm) and placed on shakers (50 rpm) at 25 to 27°C with a 16-h-light/8-h-dark photoperiod for 4 d and light intensity of 150 μmol m^{-2} s^{-1}. Twenty-four hours before treatment, TvWT was cultured in 1 L of Potato Dextrose Broth in a Fernbach flask at a concentration of 10^5 spores/mL. The mycelia were collected by filtration with sterile nylon and washed with sterile water. One gram of fresh weight of the mycelial inoculum was added to the jars, after which a second mason jar (24-oz wide mouth canning jar [Ball]) was placed atop the first jar and held in place with parafilm to allow unimpeded shoot growth. Root tissue was harvested at 6 and 54 h after adding *T. virens* inoculum to the hydroponic jars with maize seedlings. The shoot tissue included all parts above the maize mesocotyl, while the root tissue included the radicle, lateral, and seminal roots. The roots were not rinsed with water when collected, especially at 54 h when the *T. virens* tissue was inextricable from maize root tissue. All the tissue samples collected were immediately flash frozen in liquid nitrogen and preserved at −80°C until RNA extraction.

RNA Extraction and RNA-Seq Analysis

RNA was extracted from root using a modified method for the RNeasy Plant Mini kit (catalog no. 74903, QIAGEN). The tissue samples were first ground in liquid nitrogen, and 1 μg of the tissue was aliquoted for RNA extraction. While the samples were still chilled in liquid nitrogen, 1 mL of TRI reagent (catalog no. TR118, Molecular Research Center) was added to each sample and mixed well. The samples were left at room temperature for 5 min before

200 μL of chloroform was added and mixed well. The samples were stored at room temperature for 10 min before being centrifuged at 13,000*g* at 4°C for 15 min. The supernatant was transferred to a new tube containing 500 μL of isopropanol. The samples were gently mixed and stored at room temperature for 10 min prior to transfer into the RNeasy spin columns (Qiagen). The samples were then processed following the manufacturer's instructions. For each sample, 3 μg of RNA was treated with DNase I (catalog no. EN0521, Thermo Fisher Scientific) following the manufacturer's instructions. RNA-seq analysis was performed at the Texas A&M AgriLife Genomics and Bioinformatics Service. The cDNA libraries were created with the NEXTflex Rapid Illumina Directional RNA-Seq Library Prep kit (catalog no. NOVA-5138-07, Bioo Scientific). Sequencing parameters were 50-bp paired end reads, to a depth of 250 million reads, on a NovaSeq 6000 system (catalog no. 20012850, Illumina).

RNA-Seq Data Analysis

Base-calling, quality checking, and removal of adaptor sequences was performed by the Texas A&M AgriLife Genomic and Bioinformatics Service as per their standard operating procedure. Raw, paired end, 50-bp reads were then aligned back to the B73 reference genome sequence (AGPv4 release 38) via the TopHat2 v2.1.0 pipeline (Kim et al., 2013). Uniquely aligned reads were counted with the HT-Seq 0.6.1 pipeline (Anders et al., 2015) using the Ensembl GCA_000005005.6 Zm-B73-REFERENCE-GRAMENE-4.0 for annotation. The FPKM values were determined using the Ballgown (v2.10.0) pipeline (https://ccb.jhu.edu/software.shtml). The raw and processed RNA-seq data from this study have been deposited at Gene Expression Omnibus (https://www.ncbi.nlm.nih.gov/geo/).

qPCR Analysis

RNA-seq results were validated with qPCR. The qPCR reactions were set up using the Verso 1-step RT-qPCR kit, SYBR Green, ROX (catalog no. AB4106A, Thermo Fisher Scientific) following the manufacturer's procedure with 10-μL volume reactions. The samples were run in the StepOne Real-Time PCR system (catalog no. 4376357, Applied Biosystems) using the following conditions: 48°C for 30 min, 95°C for 10 min, followed by 40 cycles of 95°C for 15 s, 54°C for 30 s, 72°C for 30 s. Melt curve conditions were 95°C for 15 s, 60°C for 1 min, 95°C for 15 s. After normalizing to maize *α-TUBULIN*, relative expression was determined as fold change between untreated B73 and TvWT-treated B73 using the $2^{-\Delta\Delta CT}$ method (Czechowski et al., 2005; Xia et al., 2014). Expression of *LOX10* in B73 roots in response to treatment with TvWT, *Δsm1*, or *Δsir1* was performed in a similar manner. Expression of *T. virens SM1* and *SIR1* was normalized to *Actin*. Primers used are listed in Supplemental Table 3.

Confocal Microscopy for LOX10-YFP

Transgenic maize producing LOX10-YFP fusion proteins (Mohanty et al., 2009) were grown under hydroponic conditions as stated previously. After treatment with TvWT, roots were harvested every 12 h for 72 h, and images were collected using the Nikon FN1 C1si confocal microscope.

Statistical Analysis

Statistically significant differences were determined by one-way ANOVA followed by post hoc tests. Student's *t* test was used for comparisons between two sample groups, while Tukey honestly significant difference (HSD) test was used for other comparisons. A value of $P < 0.05$ was considered to be statistically significant. The number of biological replicates and significance thresholds for each experiment are indicated in the figure legends. Details of statistical results are in Supplemental Data Set 2.

Accession Numbers

RNA-seq data from this study can be found at Gene Expression Omnibus under accession number GSE137826. Maize gene accession numbers are listed in Supplemental Table 2.

Supplemental Data

Supplemental Figure 1. Increased root colonization of *lox10-3* by *T. virens* has no detrimental effects on plant growth and development (supports Figure 2 and 3).

Supplemental Figure 2. qPCR validation of RNA-seq transcriptomic analysis (supports Figure 10).

Supplemental Figure 3. Maize-*T. virens* interactions do not upregulate RES response genes (supports Figures 7 and 10).

Supplemental Figure 4. Metabolite profiling of seedling shoot tissue from TvWT-treated maize reveals significantly increased SA, but not 12-OPDA, KODA, JA, or JA-Ile (supports Figures 10 and 11).

Supplemental Table 1. Common and formal names, m/z, and retention times of oxylipins and phytohormones in this study.

Supplemental Table 2. IDs, names, and functions of genes in this study for the RNA-seq results.

Supplemental Table 3. List of the genes and the primer sequences for RT-qPCR used in this study.

Supplemental Data Set 1. Detected metabolites and phytohormones in collected xylem sap samples. LC-MS/MS.

Supplemental Data Set 2. Statistical Report of ANOVA Results for the data presented in each figure.

ACKNOWLEDGMENTS

We thank Pei-Cheng Huang, Zack Gorman, Nasie Constantino, Ramadhika Damarwinasis, John Bennet, James Taylor, and Robert Dorosky (Texas A&M University) for help in preparing hydroponic growth of maize and tissue harvesting. Brianna Hankinson, Joseph Vasselli, and Andrew Horgan (Texas A&M University) are acknowledged for contributions in ISR assays, xylem sap collection, xylem sap transfusions, and RNA extractions. We thank Kacey Wilson (Texas A&M University) for contributions in root colonization assays. Jordan Tolley (Texas A&M University) is acknowledged for LOX10-YFP fusion protein imaging using confocal microscopy. We thank Elizabeth Malinich for guidance on RNA-seq data analysis. We acknowledge the Texas A&M AgriLife Genomics and Bioinformatics Service for their sequencing services and the Texas A&M High Computing Research Center for providing supercomputing capability for RNA-seq analysis. This work was supported by the USDA-National Institute of Food and Agriculture (NIFA grant 2016-67013-24730 to C.M.K. and M.V.K and 2017-67013-26524 to M.V.K.).

AUTHOR CONTRIBUTIONS

K.-D.W., E.J.B., C.M.K., and M.V.K. designed the research and analyzed data; K.-D.W. performed most of the experiments; E.J.B. quantified metabolites via LC-MS/MS; and K.-D.W., C.M.K., and M.V.K. wrote the article with input from and revisions by E.J.B., C.M.K., and M.V.K.

Received June 28, 2019; revised September 30, 2019; accepted November 1, 2019; published January 4, 2019.

REFERENCES

Alméras, E., Stolz, S., Vollenweider, S., Reymond, P., Mène-Saffrané, L., and Farmer, E.E. (2003). Reactive electrophile species activate defense gene expression in Arabidopsis. Plant J. **34:** 205–216.

Alonso-Ramírez, A., Poveda, J., Martín, I., Hermosa, R., Monte, E., and Nicolás, C. (2014). Salicylic acid prevents *Trichoderma harzianum* from entering the vascular system of roots. Mol. Plant Pathol. **15:** 823–831.

An, L., Ahmad, R.M., Ren, H., Qin, J., and Yan, Y. (2018). Jasmonate signal receptor gene family ZmCOIs restore male fertility and defense response of Arabidopsis mutant *coi1–1*. J. Plant Growth Regul. **38:** 479–493.

Anders, S., Pyl, P., and Huber, W. (2015). HTSeq—a Python framework to work with high-throughput sequencing data. Bioinformatics **31:** 166–169.

Andreou, A., Brodhun, F., and Feussner, I. (2009). Biosynthesis of oxylipins in non-mammals. Prog. Lipid Res. **48:** 148–170.

Baek, J.M., and Kenerley, C.M. (1998). The *arg2* gene of *Trichoderma virens*: Cloning and development of a homologous transformation system. Fungal Genet. Biol. **23:** 34–44.

Blechert, S., Bockelmann, C., Fusslein, M., Von Schrader, T., Stelmach, B., Niesel, U., and Weiler, E.W. (1999). Structure-activity analyses reveal the existence of two separate groups of active octadecanoids in elicitation of the tendril-coiling response of *Bryonia dioica* Jacq. Planta **207:** 470–479.

Borrego, E.J., and Kolomiets, M.V. (2016). Synthesis and functions of jasmonates in maize. Plants (Basel) **5:** 41.

Christensen, S.A. (2009). The Function of the Lipoxygenase ZmLOX10 in Maize Interactions with Insects and Pathogens. PhD dissertation (College Station: Texas A&M University).

Christensen, S.A., et al. (2015). Maize death acids, 9-lipoxygenase-derived cyclopente(a)nones, display activity as cytotoxic phytoalexins and transcriptional mediators. Proc. Natl. Acad. Sci. USA **112:** 11407–11412.

Christensen, S.A., et al. (2013). The maize lipoxygenase, *ZmLOX10*, mediates green leaf volatile, jasmonate and herbivore-induced plant volatile production for defense against insect attack. Plant J. **74:** 59–73.

Christensen, S.A., Nemchenko, A., Park, Y.S., Borrego, E., Huang, P.C., Schmelz, E.A., Kunze, S., Feussner, I., Yalpani, N., Meeley, R., and Kolomiets, M.V. (2014). The novel monocot-specific 9-lipoxygenase *ZmLOX12* is required to mount an effective jasmonate-mediated defense against *Fusarium verticillioides* in maize. Mol. Plant Microbe Interact. **27:** 1263–1276.

Conrath, U., et al.; Prime-A-Plant Group (2006). Priming: Getting ready for battle. Mol. Plant Microbe Interact. **19:** 1062–1071.

Constantino, N.N., Mastouri, F., Damarwinasis, R., Borrego, E.J., Moran-Diez, M.E., Kenerley, C.M., Gao, X., and Kolomiets, M.V. (2013). Root-expressed maize lipoxygenase 3 negatively regulates induced systemic resistance to *Colletotrichum graminicola* in shoots. Front. Plant Sci. **4:** 510.

Contreras-Cornejo, H.A., Macías-Rodríguez, L., Beltrán-Peña, E., Herrera-Estrella, A., and López-Bucio, J. (2011). *Trichoderma*-induced plant immunity likely involves both hormonal- and camalexin-dependent mechanisms in *Arabidopsis thaliana* and confers resistance against necrotrophic fungi *Botrytis cinerea*. Plant Signal. Behav. **6:** 1554–1563.

Czechowski, T., Stitt, M., Altmann, T., Udvardi, M.K., and Scheible, W.-R. (2005). Genome-wide identification and testing of superior reference genes for transcript normalization in Arabidopsis. Plant Physiol. **139:** 5–17.

Dave, A., and Graham, I.A. (2012). Oxylipin signaling: A distinct role for the jasmonic acid precursor cis-(+)-12-oxo-phytodienoic acid (cis-OPDA). Front. Plant Sci. **3:** 42.

Dave, A., Hernández, M.L., He, Z., Andriotis, V.M., Vaistij, F.E., Larson, T.R., and Graham, I.A. (2011). 12-Oxo-phytodienoic acid accumulation during seed development represses seed germination in *Arabidopsis*. Plant Cell **23:** 583–599.

Djonović, S., Pozo, M.J., Dangott, L.J., Howell, C.R., and Kenerley, C.M. (2006). Sm1, a proteinaceous elicitor secreted by the biocontrol fungus *Trichoderma virens* induces plant defense responses and systemic resistance. Mol. Plant Microbe Interact. **19:** 838–853.

Djonovic, S., Vargas, W.A., Kolomiets, M.V., Horndeski, M., Wiest, A., and Kenerley, C.M. (2007). A proteinaceous elicitor Sm1 from the beneficial fungus *Trichoderma virens* is required for induced systemic resistance in maize. Plant Physiol. **145:** 875–889.

Druzhinina, I.S., Seidl-Seiboth, V., Herrera-Estrella, A., Horwitz, B.A., Kenerley, C.M., Monte, E., Mukherjee, P.K., Zeilinger, S., Grigoriev, I.V., and Kubicek, C.P. (2011). *Trichoderma*: The genomics of opportunistic success. Nat. Rev. Microbiol. **9:** 749–759.

Dubois, M., Van den Broeck, L., and Inzé, D. (2018). The pivotal role of ethylene in plant growth. Trends Plant Sci. **23:** 311–323.

Farmer, E.E., Caldelari, D., Pearce, G., Walker-Simmons, M., and Ryan, C.A. (1994). Diethyldithiocarbamic acid inhibits the octadecanoid signaling pathway for the wound induction of proteinase inhibitors in tomato leaves. Plant Physiol. **106:** 337–342.

Feussner, I., and Wasternack, C. (2002). The lipoxygenase pathway. Annu. Rev. Plant Biol. **53:** 275–297.

Floková, K., Feussner, K., Herrfurth, C., Miersch, O., Mik, V., Tarkowská, D., Strnad, M., Feussner, I., Wasternack, C., and Novák, O. (2016). A previously undescribed jasmonate compound in flowering *Arabidopsis thaliana* - The identification of cis-(+)-OPDA-Ile. Phytochemistry **122:** 230–237.

Forchetti, G., Masciarelli, O., Alemano, S., Alvarez, D., and Abdala, G. (2007). Endophytic bacteria in sunflower (*Helianthus annuus* L.): Isolation, characterization, and production of jasmonates and abscisic acid in culture medium. Appl. Microbiol. Biotechnol. **76:** 1145–1152.

Gao, X., Shim, W.B., Göbel, C., Kunze, S., Feussner, I., Meeley, R., Balint-Kurti, P., and Kolomiets, M. (2007). Disruption of a maize 9-lipoxygenase results in increased resistance to fungal pathogens and reduced levels of contamination with mycotoxin fumonisin. Mol. Plant Microbe Interact. **20:** 922–933.

Gao, X., Starr, J., Göbel, C., Engelberth, J., Feussner, I., Tumlinson, J., and Kolomiets, M. (2008). Maize 9-lipoxygenase *ZmLOX3* controls development, root-specific expression of defense genes, and resistance to root-knot nematodes. Mol. Plant Microbe Interact. **21:** 98–109.

Gleason, C., Leelarasamee, N., Meldau, D., and Feussner, I. (2016). OPDA has key role in regulating plant susceptibility to the root-knot nematode *Meloidogyne hapla* in *Arabidopsis*. Front. Plant Sci. **7:** 1565.

Goetz, S., Hellwege, A., Stenzel, I., Kutter, C., Hauptmann, V., Forner, S., McCaig, B., Hause, G., Miersch, O., Wasternack, C., and Hause, B. (2012). Role of cis-12-oxo-phytodienoic acid in tomato embryo development. Plant Physiol. **158:** 1715–1727.

Guo, H.M., Li, H.C., Zhou, S.R., Xue, H.W., and Miao, X.X. (2014). Cis-12-oxo-phytodienoic acid stimulates rice defense response to a piercing-sucking insect. Mol. Plant **7:** 1683–1692.

Haque, E., Osmani, A.A., Ahmadi, S.H., Ogawa, S., Takagi, K., Yokoyama, M., and Ban, T. (2016). KODA, an α-ketol derivative of linolenic acid provides wide recovery ability of wheat against various abiotic stresses. Biocatal. Agric. Biotechnol. **7:** 67–75.

Havko, N.E., Major, I.T., Jewell, J.B., Attaran, E., Browse, J., and Howe, G.A. (2016). Control of carbon assimilation and partitioning by jasmonate: An accounting of growth–defense tradeoffs. Plants (Basel) **5:** 7.

Heil, M., and Bostock, R.M. (2002). Induced systemic resistance (ISR) against pathogens in the context of induced plant defences. Ann. Bot. **89:** 503–512.

Hermosa, R., Viterbo, A., Chet, I., and Monte, E. (2012). Plant-beneficial effects of *Trichoderma* and of its genes. Microbiology **158:** 17–25.

Hossain, M.M., Sultana, F., and Hyakumachi, M. (2017). Role of ethylene signalling in growth and systemic resistance induction by the plant growth-promoting fungus *Penicillium viridicatum* in Arabidopsis. J. Phytopathol. **165:** 432–441.

Howe, G.A., Lightner, J., Browse, J., and Ryan, C.A. (1996). An octadecanoid pathway mutant (JL5) of tomato is compromised in signaling for defense against insect attack. Plant Cell **8:** 2067–2077.

Howe, G.A., and Schilmiller, A.L. (2002). Oxylipin metabolism in response to stress. Curr. Opin. Plant Biol. **5:** 230–236.

Howell, C.R., Hanson, L.E., Stipanovic, R.D., and Puckhaber, L.S. (2000). Induction of terpenoid synthesis in cotton roots and control of rhizoctonia solani by seed treatment with *Trichoderma virens*. Phytopathology **90:** 248–252.

Huang, H., Liu, B., Liu, L., and Song, S. (2017). Jasmonate action in plant growth and development. J. Exp. Bot. **68:** 1349–1359.

Huot, B., Yao, J., Montgomery, B.L., and He, S.Y. (2014). Growth-defense tradeoffs in plants: A balancing act to optimize fitness. Mol. Plant **7:** 1267–1287.

Iavicoli, A., Boutet, E., Buchala, A., and Métraux, J.-P. (2003). Induced systemic resistance in *Arabidopsis thaliana* in response to root inoculation with *Pseudomonas fluorescens* CHA0. Mol. Plant Microbe Interact. **16:** 851–858.

Isakeit, T., Gao, X., and Kolomiets, M. (2007). Increased resistance of a maize mutant lacking the 9-lipoxygenase gene, *ZmLOX3*, to root rot caused by *Exserohilum pedicellatum*. J. Phytopathol. **155:** 758–760.

Jogaiah, S., Abdelrahman, M., Tran, L.P., and Ito, S.I. (2018). Different mechanisms of *Trichoderma virens*-mediated resistance in tomato against Fusarium wilt involve the jasmonic and salicylic acid pathways. Mol. Plant Pathol. **19:** 870–882.

Katagiri, F., and Tsuda, K. (2010). Understanding the plant immune system. Mol. Plant Microbe Interact. **23:** 1531–1536.

Kim, D., Pertea, G., Trapnell, C., Pimentel, H., Kelley, R., and Salzberg, S. (2013). TopHat2: Accurate alignment of transcriptomes in the presence of insertions, deletions and gene fusions. Genome biology **14:** R36.

Kittikorn, M., Shiraishi, N., Okawa, K., Ohara, H., Yokoyama, M., Ifuku, O., Yoshida, S., and Kondo, S. (2010). Effect of fruit load on 9,10-ketol-octadecadienoic acid (KODA), GA and jasmonic acid concentrations in apple buds. Sci. Hortic. **124:** 225–230.

Klessig, D.F., Choi, H.W., and Dempsey, D.A. (2018). Systemic acquired resistance and salicylic acid: Past, present, and future. Mol. Plant Microbe Interact. **31:** 871–888.

Knoester, M., Pieterse, C.M.J., Bol, J.F., and Van Loon, L.C. (1999). Systemic resistance in *Arabidopsis* induced by rhizobacteria requires ethylene-dependent signaling at the site of application. Mol. Plant Microbe Interact. **12:** 720–727.

Korolev, N., David, D.R., and Elad, Y. (2008). The role of phytohormones in basal resistance and *Trichoderma*-induced systemic resistance to *Botrytis cinerea* in *Arabidopsis thaliana*. BioControl **53:** 667–683.

Lamdan, N.L., Shalaby, S., Ziv, T., Kenerley, C.M., and Horwitz, B.A. (2015). Secretome of *Trichoderma* interacting with maize roots: Role in induced systemic resistance. Mol. Cell. Proteomics **14:** 1054–1063.

Li, C., Liu, G., Xu, C., Lee, G.I., Bauer, P., Ling, H.Q., Ganal, M.W., and Howe, G.A. (2003). The tomato suppressor of prosystemin-mediated responses2 gene encodes a fatty acid desaturase required for the biosynthesis of jasmonic acid and the production of a systemic wound signal for defense gene expression. Plant Cell **15:** 1646–1661.

Lorito, M., Woo, S.L., Harman, G.E., and Monte, E. (2010). Translational research on *Trichoderma*: From 'omics to the field. Annu. Rev. Phytopathol. **48:** 395–417.

Lunde, C., Kimberlin, A., Leiboff, S., Koo, A.J., and Hake, S. (2019). *Tasselseed5* overexpresses a wound-inducible enzyme, *ZmCYP94B1*, that affects jasmonate catabolism, sex determination, and plant architecture in maize. Commun. Biol **2:** 114.

Luo, Z.-B., Janz, D., Jiang, X., Göbel, C., Wildhagen, H., Tan, Y., Rennenberg, H., Feussner, I., and Polle, A. (2009). Upgrading root physiology for stress tolerance by ectomycorrhizas: Insights from metabolite and transcriptional profiling into reprogramming for stress anticipation. Plant Physiol. **151:** 1902–1917.

Malinich, E.A., Wang, K., Mukherjee, P.K., Kolomiets, M., and Kenerley, C.M. (2019). Differential expression analysis of *Trichoderma virens* RNA reveals a dynamic transcriptome during colonization of *Zea mays* roots. BMC Genomics **20:** 280.

Martínez-Medina, A., Appels, F.V.W., and van Wees, S.C.M. (2017). Impact of salicylic acid- and jasmonic acid-regulated defences on root colonization by *Trichoderma harzianum* T-78. Plant Signal. Behav. **12:** e1345404.

Maynard, D., Gröger, H., Dierks, T., and Dietz, K.J. (2018). The function of the oxylipin 12-oxophytodienoic acid in cell signaling, stress acclimation, and development. J. Exp. Bot. **69:** 5341–5354.

Mohanty, A., Luo, A., DeBlasio, S., Ling, X., Yang, Y., Tuthill, D.E., Williams, K.E., Hill, D., Zadrozny, T., Chan, A., Sylvester, A.W., and Jackson, D. (2009). Advancing cell biology and functional genomics in maize using fluorescent protein-tagged lines. Plant Physiol. **149:** 601–605.

Monte, I., et al. (2018). Ligand-receptor co-evolution shaped the jasmonate pathway in land plants. Nat. Chem. Biol. **14:** 480–488.

Mueller, S., Hilbert, B., Dueckershoff, K., Roitsch, T., Krischke, M., Mueller, M.J., and Berger, S. (2008). General detoxification and stress responses are mediated by oxidized lipids through TGA transcription factors in *Arabidopsis*. Plant Cell **20:** 768–785.

Mukherjee, P.K., and Kenerley, C.M. (2010). Regulation of morphogenesis and biocontrol properties in *Trichoderma virens* by a VELVET protein, Vel1. Appl. Environ. Microbiol. **76:** 2345–2352.

Müller, M., and Munné-Bosch, S. (2011). Rapid and sensitive hormonal profiling of complex plant samples by liquid chromatography coupled to electrospray ionization tandem mass spectrometry. Plant Methods **7:** 37.

Navarro-Meléndez, A.L., and Heil, M. (2014). Symptomless endophytic fungi suppress endogenous levels of salicylic acid and interact with the jasmonate-dependent indirect defense traits of their host, lima bean (*Phaseolus lunatus*). J. Chem. Ecol. **40:** 816–825.

Nemchenko, A., Kunze, S., Feussner, I., and Kolomiets, M. (2006). Duplicate maize 13-lipoxygenase genes are differentially regulated by circadian rhythm, cold stress, wounding, pathogen infection, and hormonal treatments. J. Exp. Bot. **57:** 3767–3779.

Oliw, E.H., and Hamberg, M. (2017). An allene oxide and 12-oxophytodienoic acid are key intermediates in jasmonic acid biosynthesis by *Fusarium oxysporum*. J. Lipid Res. **58:** 1670–1680.

Park, Y.-H., Stack, J., and Kenerley, C. (1992). Selective isolation and enumeration of *Gliocladium virens* and *G. roseum* from soil. Plant Dis. **76:** 230–235.

Pieterse, C.M., Van der Does, D., Zamioudis, C., Leon-Reyes, A., and Van Wees, S.C. (2012). Hormonal modulation of plant immunity. Annu. Rev. Cell Dev. Biol. **28:** 489–521.

Pieterse, C.M., van Wees, S.C., van Pelt, J.A., Knoester, M., Laan, R., Gerrits, H., Weisbeek, P.J., and van Loon, L.C. (1998). A novel

signaling pathway controlling induced systemic resistance in *Arabidopsis*. Plant Cell **10:** 1571–1580.

Pieterse, C.M., Zamioudis, C., Berendsen, R.L., Weller, D.M., Van Wees, S.C., and Bakker, P.A. (2014b). Induced systemic resistance by beneficial microbes. Annu. Rev. Phytopathol. **52:** 347–375.

Pieterse, C.M., Zamioudis, C., Does, D., and Van Wees, S.C. (2014a). Signalling networks involved in induced resistance. In . In Induced Resistance for Plant Defence: A Sustainable Approach to Crop Protection, D. Walters, A.C. Newton, and and G. Lyon, eds, . (New York: John Wiley and Sons), pp. 58–80.

Plett, J.M., Daguerre, Y., Wittulsky, S., Vayssières, A., Deveau, A., Melton, S.J., Kohler, A., Morrell-Falvey, J.L., Brun, A., Veneault-Fourrey, C., and Martin, F. (2014). Effector MiSSP7 of the mutualistic fungus *Laccaria bicolor* stabilizes the *Populus* JAZ6 protein and represses jasmonic acid (JA) responsive genes. Proc. Natl. Acad. Sci. USA **111:** 8299–8304.

Plett, J.M., Kemppainen, M., Kale, S.D., Kohler, A., Legué, V., Brun, A., Tyler, B.M., Pardo, A.G., and Martin, F. (2011). A secreted effector protein of *Laccaria bicolor* is required for symbiosis development. Curr. Biol. **21:** 1197–1203.

Ponce De León, I., Schmelz, E.A., Gaggero, C., Castro, A., Álvarez, A., and Montesano, M. (2012). *Physcomitrella patens* activates reinforcement of the cell wall, programmed cell death and accumulation of evolutionary conserved defence signals, such as salicylic acid and 12-oxo-phytodienoic acid, but not jasmonic acid, upon *Botrytis cinerea* infection. Mol. Plant Pathol. **13:** 960–974.

Pozo, M.J., Van Der Ent, S., Van Loon, L.C., and Pieterse, C.M. (2008). Transcription factor MYC2 is involved in priming for enhanced defense during rhizobacteria-induced systemic resistance in *Arabidopsis thaliana*. New Phytol. **180:** 511–523.

Prost, I., et al. (2005). Evaluation of the antimicrobial activities of plant oxylipins supports their involvement in defense against pathogens. Plant Physiol. **139:** 1902–1913.

Sakamoto, D., Nakamura, Y., Sugiura, H., Sugiura, T., Asakura, T., Yokoyama, M., and Moriguchi, T. (2010). Effect of 9-hydroxy-10-oxo-12(Z), 15(Z)-octadecadienoic acid (KODA) on endodormancy breaking in flower buds of japanese pear. HortScience **45:** 1470–1474.

Salas-Marina, M.A., Isordia-Jasso, M.I., Islas-Osuna, M.A., Delgado-Sánchez, P., Jiménez-Bremont, J.F., Rodríguez-Kessler, M., Rosales-Saavedra, M.T., Herrera-Estrella, A., and Casas-Flores, S. (2015). The Epl1 and Sm1 proteins from *Trichoderma atroviride* and *Trichoderma virens* differentially modulate systemic disease resistance against different life style pathogens in *Solanum lycopersicum*. Front. Plant Sci. **6:** 77.

Salas-Marina, M.A., Silva-Flores, M.A., Uresti-Rivera, E.E., Castro-Longoria, E., Herrera-Estrella, A., and Casas-Flores, S. (2011). Colonization of *Arabidopsis* roots by *Trichoderma atroviride* promotes growth and enhances systemic disease resistance through jasmonic acid/ethylene and salicylic acid pathways. Eur. J. Plant Pathol. **131:** 15–26.

Scalschi, L., Sanmartín, M., Camañes, G., Troncho, P., Sánchez-Serrano, J.J., García-Agustín, P., and Vicedo, B. (2015). Silencing of OPR3 in tomato reveals the role of OPDA in callose deposition during the activation of defense responses against *Botrytis cinerea*. Plant J. **81:** 304–315.

Shoresh, M., Yedidia, I., and Chet, I. (2005). Involvement of jasmonic acid/ethylene signaling pathway in the systemic resistance induced in cucumber by *Trichoderma asperellum* T203. Phytopathology **95:** 76–84.

Song, S., Qi, T., Fan, M., Zhang, X., Gao, H., Huang, H., Wu, D., Guo, H., and Xie, D. (2013). The bHLH subgroup IIId factors negatively regulate jasmonate-mediated plant defense and development. PLoS Genet. **9:** e1003653.

Song, Y., Chen, D., Lu, K., Sun, Z., and Zeng, R. (2015). Enhanced tomato disease resistance primed by arbuscular mycorrhizal fungus. Front. Plant Sci. **6:** 786.

Stelmach, B.A., Müller, A., Hennig, P., Laudert, D., Andert, L., and Weiler, E.W. (1998). Quantitation of the octadecanoid 12-oxo-phytodienoic acid, a signalling compound in plant mechanotransduction. Phytochemistry **47:** 539–546.

Stumpe, M., Göbel, C., Faltin, B., Beike, A.K., Hause, B., Himmelsbach, K., Bode, J., Kramell, R., Wasternack, C., Frank, W., Reski, R., and Feussner, I. (2010). The moss *Physcomitrella patens* contains cyclopentenones but no jasmonates: Mutations in allene oxide cyclase lead to reduced fertility and altered sporophyte morphology. New Phytol. **188:** 740–749.

Taki, N., et al. (2005). 12-Oxo-phytodienoic acid triggers expression of a distinct set of genes and plays a role in wound-induced gene expression in *Arabidopsis*. Plant Physiol. **139:** 1268–1283.

Tjamos, S.E., Flemetakis, E., Paplomatas, E.J., and Katinakis, P. (2005). Induction of resistance to *Verticillium dahliae* in *Arabidopsis thaliana* by the biocontrol agent K-165 and pathogenesis-related proteins gene expression. Mol. Plant Microbe Interact. **18:** 555–561.

Tsukada, K., Takahashi, K., and Nabeta, K. (2010). Biosynthesis of jasmonic acid in a plant pathogenic fungus, *Lasiodiplodia theobromae*. Phytochemistry **71:** 2019–2023.

Tzeng, T.H., Lyngholm, L.K., Ford, C.F., and Bronson, C.R. (1992). A restriction fragment length polymorphism map and electrophoretic karyotype of the fungal maize pathogen *Cochliobolus heterostrophus*. Genetics **130:** 81–96.

Varsani, S., Grover, S., Zhou, S., Koch, K.G., Huang, P.-C., Kolomiets, M.V., Williams, W.P., Heng-Moss, T., Sarath, G., Luthe, D.S., Jander, G., and Louis, J. (2019). 12-Oxo-phytodienoic acid acts as a regulator of maize defense against corn leaf aphid. Plant Physiol. **179:** 1402–1415.

Vick, B.A., and Zimmerman, D.C. (1984). Biosynthesis of jasmonic acid by several plant species. Plant Physiol. **75:** 458–461.

Wang, K., Guo, Q., Froehlich, J.E., Hersh, H.L., Zienkiewicz, A., Howe, G.A., and Benning, C. (2018). Two abscisic acid-responsive plastid lipase genes involved in jasmonic acid biosynthesis in *Arabidopsis thaliana*. Plant Cell **30:** 1006–1022.

Wang, S., Saito, T., Ohkawa, K., Ohara, H., Shishido, M., Ikeura, H., Takagi, K., Ogawa, S., Yokoyama, M., and Kondo, S. (2016). α-Ketol linolenic acid (KODA) application affects endogenous abscisic acid, jasmonic acid and aromatic volatiles in grapes infected by a pathogen (*Glomerella cingulata*). J. Plant Physiol. **192:** 90–97.

Wang, Y., Ohara, Y., Nakayashiki, H., Tosa, Y., and Mayama, S. (2005). Microarray analysis of the gene expression profile induced by the endophytic plant growth-promoting rhizobacteria, *Pseudomonas fluorescens* FPT9601-T5 in *Arabidopsis*. Mol. Plant Microbe Interact. **18:** 385–396.

Wasternack, C. (2007). Jasmonates: An update on biosynthesis, signal transduction and action in plant stress response, growth and development. Ann. Bot. **100:** 681–697.

Wasternack, C., and Hause, B. (2013). Jasmonates: Biosynthesis, perception, signal transduction and action in plant stress response, growth and development. An update to the 2007 review in Annals of Botany. Ann. Bot. **111:** 1021–1058.

Xia, A., Feng-ying, D., Song, G., Fan-jun, C., Li-Xing, Y., and Ri-Liang, G. (2014). Transcriptional regulation of expression of the maize aldehyde dehydrogenase 7 gene (ZmALDH7B6) in response to abiotic stresses. J. Integr. Agric. **13:** 1900–1908.

Yamamoto, Y., Ohshika, J., Takahashi, T., Ishizaki, K., Kohchi, T., Matusuura, H., and Takahashi, K. (2015). Functional analysis of allene oxide cyclase, MpAOC, in the liverwort *Marchantia polymorpha*. Phytochemistry **116:** 48–56.

Yan, Y., Christensen, S., Isakeit, T., Engelberth, J., Meeley, R., Hayward, A., Emery, R.J., and Kolomiets, M.V. (2012). Disruption of OPR7 and OPR8 reveals the versatile functions of jasmonic acid in maize development and defense. Plant Cell **24:** 1420–1436.

Yedidia, I., Benhamou, N., and Chet, I. (1999). Induction of defense responses in cucumber plants (*Cucumis sativus* L.) by the biocontrol agent *trichoderma harzianum*. Appl. Environ. Microbiol. **65:** 1061–1070.

Yokoyama, M., Yamaguchi, S., Inomata, S., Komatsu, K., Yoshida, S., Iida, T., Yokokawa, Y., Yamaguchi, M., Kaihara, S., and Takimoto, A. (2000). Stress-induced factor involved in flower formation of *Lemna* is an α-ketol derivative of linolenic acid. Plant Cell Physiol. **41:** 110–113.